

1 **Unexpectedly low recombination rates and presence of hotspots in termite genomes**

2

3 Turid Everitt^{1#}, Tilman Rönneburg^{1#}, Daniel Elsner², Anna Olsson¹, Yuanzhen Liu¹, Tuuli
4 Larva¹, Judith Korb^{2,3}, Matthew T Webster^{1,4*}

5

6 1) Medical Biochemistry and Microbiology, Uppsala University, Uppsala, Sweden

7 2) Evolutionary Biology and Ecology, University of Freiburg, Freiburg, Germany

8 3) Research Institute for the Environment and Livelihoods, Charles Darwin University,

9 Casuarina Campus, Darwin, Australia

10 4) Science for Life Laboratory, Uppsala University, Uppsala, Sweden

11 # equal contribution

12

13 *correspondence to matthew.webster@imbim.uu.se

14

15 **Abstract**

16 Meiotic recombination is a fundamental evolutionary process that facilitates adaptation and
17 the removal of deleterious genetic variation. Social Hymenoptera exhibit some of the
18 highest recombination rates among metazoans, whereas high recombination rates have not
19 been found among non-social species from this insect order. It is unknown whether
20 elevated recombination rates are a ubiquitous feature of all social insects. In many
21 metazoan taxa, recombination is mainly restricted to hotspots a few kilobases in length.
22 However, little is known about the prevalence of recombination hotspots in insect genomes.
23 Here we infer recombination rate and its fine-scale variation across the genomes of two
24 social species from the insect order Blattodea: the termites *Macrotermes bellicosus* and
25 *Cryptotermes secundus*. We used linkage-disequilibrium-based methods to infer
26 recombination rate. We infer that recombination rates are close to 1 cM/Mb in both
27 species, similar to the average metazoan rate. We also observed a highly punctate
28 distribution of recombination in both termite genomes, indicative of the presence of
29 recombination hotspots. We infer the presence of full-length *PRDM9* genes in the genomes
30 of both species, which suggests recombination hotspots in termites might be determined by
31 *PRDM9*, as they are in mammals. We also find that recombination rates in genes are
32 correlated with inferred levels of germline DNA methylation. The finding of low
33 recombination rates in termites indicates that eusociality is not universally connected to
34 elevated recombination rate. We speculate that the elevated recombination rates in social
35 Hymenoptera are instead promoted by intense selection among haploid males.

36

37 **Introduction**

38 Meiotic recombination has two fundamental roles: It is essential for correct disjunction of
39 chromosomes during cell division and it generates new combinations of genetic variants
40 that form the raw material of evolution (Hartfield and Keightley 2012). However,
41 recombination can also be deleterious, as it can generate structural mutations and break up
42 favourable combinations of alleles. Recombination varies among species, with optimal
43 recombination rate in a genome likely determined by the optimal trade-off of its positive
44 and negative evolutionary and mechanistic effects (Stapley et al. 2017).

45 The highest recombination rates in metazoans observed so far are found in social insects
46 (Wilfert et al. 2007; Stapley et al. 2017). However, until now recombination rate has only
47 been studied in social insects from the order Hymenoptera, to which the majority of social
48 insects belong. Among Hymenoptera, the highest rates are found in the genus *Apis*: the
49 Western honey bee *Apis mellifera* (20.8 cM/Mb) and its relatives *Apis cerana* (17.4 cM/Mb),
50 *Apis florea* (20.8 cM/Mb) and *Apis dorsata* (25.1 cM/Mb) (Beye et al. 2006; Shi et al. 2013;
51 Liu et al. 2015; Wallberg et al. 2015; Rueppell et al. 2016; Kawakami et al. 2019). Other
52 social Hymenoptera also have high rates including the bumblebee *Bombus terrestris* (8.9
53 cM/Mb) (Liu et al. 2017; Kawakami et al. 2019), the stingless bee *Frieseomelitta varia* (9.3 –
54 12.5 cM/Mb) (Waiker et al. 2021), the wasp *Vespula vulgaris* (9.7 cM/Mb) (Sirviö et al.
55 2011a) and the ants *Pogonomyrmex rugosus* (11.1 cM/Mb) (Sirviö et al. 2011b) and
56 *Acromyrmex echinaior* (6.1 cM/Mb) (Sirviö et al. 2006). In contrast, the solitary bee
57 *Megachile rotundata* and the solitary wasp *Nasonia* have relatively low rates (1.0 and 1.5
58 cM/Mb, respectively) (Niehuis et al. 2010; Jones et al. 2019). For comparison, the average
59 recombination rate of 15 insect species outside of Hymenoptera is 2.2 cM/Mb (Wilfert et al.
60 2007).

61 We can learn about the forces shaping the evolution of recombination rates in general by
62 understanding why high recombination rates have evolved in social Hymenoptera. Several
63 hypotheses have been proposed to explain this observation. One set of explanations
64 focusses on the effects of recombination on intra-colony genetic diversity. For example,
65 increasing the genetic diversity of a colony could promote task specialization among
66 workers (Kent et al. 2012; Kent and Zayed 2013). Similarly, elevated genetic variation in a
67 colony could prevent invasion by pathogens or parasites due to diversification of immune
68 genes (Fischer and Schmid-Hempel 2005). Recombination could also reduce variance in
69 relatedness between nestmates, thereby reducing potential kin conflict within colonies
70 (Sherman 1979; Templeton 1979; Wilfert et al. 2007). Additionally, it has been proposed
71 that high recombination rates could have facilitated the evolution of eusociality over a
72 longer evolutionary timescale, because recombination between genes that take on
73 functions in different castes permits them to evolve more independently (Kent and Zayed
74 2013). Several studies have addressed these hypotheses (Kent et al. 2012; Liu et al. 2015;
75 Wallberg et al. 2015; Rueppell et al. 2016; Liu et al. 2017; Jones et al. 2019; Waiker et al.

76 2021; Kawakami et al. 2019) but so far none is strongly supported. It is also not clear
77 whether eusociality *per se* selects for higher recombination rates, or whether high rates are
78 a specific feature of eusocial Hymenoptera.

79 The main characteristics of eusocial insect species are the presence of castes that forgo
80 reproduction in order to care for brood or defend other colony members (workers and
81 soldiers). Eusocial insects are found mainly in Hymenoptera, among bees, wasps and ants,
82 and also Blattodea, in which all termites (Infraorder: Isoptera) are eusocial but exhibit
83 varying levels of social complexity. These insect orders likely diverged ~400 million years ago
84 (Misof et al. 2014) and there are substantial differences between social insects from the two
85 orders (Korb 2008; Korb and Thorne 2017). Hymenoptera belong to the superorder
86 Holometabola, which is the most diverse insect superorder and contains 11 orders including
87 Lepidoptera (butterflies, moths), Coleoptera (beetles), and Diptera (true flies), which all
88 undergo complete metamorphosis. Blattodea is a hemimetabolous order, which undergoes
89 partial metamorphosis. Hymenoptera have haplodiploid sex determination in which males
90 develop from haploid, unfertilized eggs and females derive from diploid, fertilized eggs. In
91 Blattodea, both males and females are diploid. Members of the worker caste in eusocial
92 Hymenoptera are all female, whereas eusocial Blattodea workers are of both sexes.
93 Hymenoptera colonies are headed by one or a small number of queens, whereas Blattodea
94 colonies contain both a king and a queen.

95 The hypotheses proposed to explain the high recombination rates observed in eusocial
96 Hymenoptera predict that recombination should be elevated in all social insects. However,
97 so far it is unknown whether social insects from other orders also have high rates. As
98 described above, there are fundamental differences in the sex determination system and
99 colony compositions of social insects from Hymenoptera and Blattodea. The robustness of
100 the association between eusociality and high recombination rates can therefore be
101 addressed by assessing mean genomic recombination rates in social Blattodea (termites).

102 In addition to variation between species, the rate of recombination also varies along
103 chromosomes. In mammals, crossover events are mainly restricted to regions that contain
104 specific motifs that act as binding sites for the PRDM9 (PR/SET domain 9) protein that marks
105 regions for double-stranded breaks, which are repaired by recombination during meiosis
106 (Baudat et al. 2010; Myers et al. 2010; Parvanov et al. 2010). Species with an active PRDM9

107 protein include nearly all mammals and many vertebrate taxa (Baker et al. 2017). In species
108 without PRDM9, recombination can be directed to hotspots defined by other features, such
109 as CpG islands and promoters that have open chromatin. Such hotspots have been
110 characterised in the genomes of diverse taxa including yeast, birds, and dogs (Axelsson et al.
111 2012; Lam and Keeney 2015; Singhal et al. 2015; Berglund et al. 2014). In insects, the
112 prevalence of recombination hotspots is not well studied. Fine-scale recombination maps in
113 the fruit fly *Drosophila melanogaster* and honey bee *A. mellifera* indicate a paucity of
114 recombination hotspots (Chan et al. 2012; Smukowski Heil et al. 2015; Wallberg et al. 2015),
115 whereas hotspots appear to be present in the genome of the butterfly *Leptidea sinapis*
116 (Torres et al. 2023).

117 Several other factors may also modulate recombination rate along chromosomes, such as
118 germline DNA methylation. Many vertebrate species have elevated recombination in CpG
119 islands, which are usually unmethylated in the germline (Axelsson et al. 2012; Singhal et al.
120 2015; Berglund et al. 2014). In insect genomes, methylation is not always present, but
121 commonly restricted to gene bodies (Arsala et al. 2022; Wang et al. 2013; Lyko et al. 2010;
122 Ventós-Alfonso et al. 2020; Bewick et al. 2019; Harrison et al. 2018). In the honey bee *A.*
123 *mellifera* and solitary bee *M. rotundata*, recombination is reduced in genes, particularly
124 those inferred to have the highest levels of germline methylation (Wallberg et al. 2015;
125 Jones et al. 2019). In addition, some studies have identified correlations between caste-
126 biases in gene expression and recombination. In honey bees, genes with worker-biased gene
127 expression have been found to have elevated recombination rates (Kent et al. 2012) but this
128 is likely an indirect result of differences in germline methylation between sets of genes
129 (Wallberg et al. 2015).

130 Here we estimate recombination rate and its fine-scale variation across the genomes of two
131 distantly related termite species with contrasting social complexities (Korb and Hartfelder
132 2008; Korb and Thorne 2017). *Macrotermes bellicosus* (Termitidae: Macrotermitinae) is a
133 fungus-growing termite with a high level of social complexity, with colonies of several
134 millions of individuals and sterile workers. It belongs to the foraging (multiple-pieces
135 nesting) termites, where workers leave the nest to forage for food. The drywood termite
136 *Cryptotermes secundus* (Kalotermitidae) has a low level of social complexity. Its colonies
137 consist of a few hundred individuals and totipotent workers from which queens and kings

138 develop (Hoffmann et al. 2012). It belongs to the wood-dwelling (one-piece nesting)
139 termites that nest in a single piece of wood that also serves as their food source.

140 The study has three main aims. Firstly, we aim to test the robustness of the association
141 between sociality and high recombination rate. If sociality is a universal driver of high
142 recombination rates, we would expect both termite species to have elevated recombination
143 rates, and that it is particularly elevated in *M. bellicosus*, which has a higher level of social
144 complexity. Secondly, we aim to determine whether recombination hotspots exist in the
145 two termite genomes, and infer whether active full-length *PRDM9* genes are present in their
146 genomes. Thirdly, we aim to analyse the factors that govern recombination rate variation
147 across the genome, in particular whether it is associated with patterns of methylation and
148 gene expression as has been reported in other studies.

149

150 **Results**

151 *Genetic variation in two termite species is typical for social insects*

152 We utilized genome assemblies of two termite species: *M. bellicosus* and *C. secundus*. The
153 genome assembly of *M. bellicosus* (Qiu et al. 2023) is 1.3 Gbp in total length across 275
154 scaffolds with scaffold N50 of 22.4 Mbp. The genome assembly of *C. secundus* (Csec_1.0)
155 (Harrison et al. 2018) is divided into 55,483 scaffolds with a scaffold N50 of 1.2 Mbp and a
156 total length of 1.0 Gbp.

157 We sequenced 10 unrelated individuals each of *M. bellicosus* and *C. secundus* to a mean
158 depth of 34x and 31x per sample, respectively (Supplemental Table S1). We mapped reads
159 to the appropriate genome assemblies and called variants in each species. In *M. bellicosus*
160 we called 5.6 million SNPs and in *C. secundus* 15.1 million SNPs (Table 1). One individual of
161 *C. secundus* (CS_8) was excluded due to a low proportion of mapped reads, poor mapping
162 quality and strand bias in mapping. Estimates of variation based on θ_w per bp (Watterson
163 1975) are 0.14% and 0.44% in *M. bellicosus* and *C. secundus* respectively, which are broadly
164 comparable to levels of variation in the honey bee *A. mellifera* (0.3 - 0.8%) (Wallberg et al.
165 2014).

166 We used these estimates of genetic variation to estimate effective population size (N_E) for
167 each of the sampled populations (Table 1). These rely on an estimate of mutation rate, μ , in

168 each species. As there is no estimate of μ for Blattodea, we considered a range of estimates
169 from insects compiled by (Lynch et al. 2023) based on experimental assays that includes
170 estimates from Diptera (*Drosophila*) (Keightley et al. 2009, 2014), Hymenoptera (Liu et al.
171 2017; Yang et al. 2015) and Lepidoptera (Keightley et al. 2015). These estimates range
172 between a minimum of $2.7 \times 10^{-10} \text{ bp}^{-1}\text{gen}^{-1}$ in *Acyrtosiphon pisum* (Fazalova and Nevado
173 2020) to a maximum of $8.1 \times 10^{-9} \text{ bp}^{-1}\text{gen}^{-1}$ in *Drosophila pseudoobscura* (Krasovec 2021).
174 The average of multiple estimates in *Drosophila melanogaster* is $4.5 \times 10^{-9} \text{ bp}^{-1}\text{gen}^{-1}$, which is
175 typical of insects (Lynch et al. 2023). A mutation rate of $\mu = 1.85 \times 10^{-9} \text{ bp}^{-1}\text{gen}^{-1}$ has been
176 estimated in the orchid mantis, *Hymenopus coronatus* (Huang et al. 2023) based on
177 inference from levels of interspecific divergence. This species is a member of the order
178 Mantodea, which contains the closest relatives of Blattodea.

179 Our estimates of N_E based on θ_W and the various mutation rates are $\sim 43,000 - 1,279,000$ in
180 *M. bellicosus*, which has high social complexity, and $\sim 137,000 - 4,081,000$ in *C. secundus*,
181 which has a lower level of social complexity (Table 1). Estimates of N_E assuming the typical
182 mutation rate of $4.5 \times 10^{-9} \text{ bp}^{-1}\text{gen}^{-1}$ are 77,000 and 245,000 respectively. Assuming the
183 mutation rate of *H. coronatus* gives an N_E of 187,000 for *M. bellicosus* and 596,000 for *C.*
184 *secundus*. These estimates are consistent with previous evidence that eusocial species with
185 large colonies and high social complexity tend to have lower effective population sizes and
186 the values are broadly comparable to levels of N_E found in social and solitary Hymenoptera
187 (Leffler et al. 2012; Romiguier et al. 2014).

188 *Low average recombination rate in termite genomes*

189 We next examined the decay of linkage disequilibrium (LD) based on the statistic r^2 . Both
190 termite species show more extensive LD compared to *A. mellifera*, which has an extremely
191 high recombination rate (Wallberg et al. 2015) (Figure 1). As N_E is broadly similar in all these
192 species, these differences are expected to largely represent differences in recombination
193 rates, and indicate that the two termite species do not exhibit the elevated genome average
194 recombination rate that is observed in honey bees.

195 We estimated variation in the population recombination rate, ρ , in both datasets using
196 LDhelmet (Chan et al. 2012) and LDhat (Auton and McVean 2007) (Table 1). Average rates of
197 ρ/kbp in *M. bellicosus* and *C. secundus* are 1.7 and 4.8 respectively from LDhat and 4.28 and

198 16.39 respectively from LDhelmet. These estimates can be converted to cM/Mb using
199 estimates of N_E , which gives average recombination rates of 0.033 - 0.986 cM/Mb in *M.*
200 *bellicosus* and 0.030 - 0.885 cM/Mb in *C. secundus* from LDhat and 0.084-2.49 cM/Mb for *M.*
201 *bellicosus* and 0.1 - 2.99 cM/Mb for *C. secundus* from LDhelmet. Using a mutation rate close
202 to the average for insects, the recombination rates in *M. bellicosus* and *C. secundus* are
203 0.550 and 0.494 cM/Mb respectively from LDhat and 1.39 and 1.67 cM/Mb respectively
204 from LDhelmet. Using the mutation rate from *H. coronatus*, the recombination rates are
205 0.23 and 0.20 cM/Mb from LDhat and 0.57 and 0.69 cM/Mb from LDhelmet for *M. bellicosus*
206 and *C. secundus*, respectively. Even though these estimates vary depending on the
207 algorithm used for estimating ρ and the assumed mutation rate, they are all substantially
208 lower than estimates from eusocial Hymenoptera (6-25 cM/Mb; (Sirviö et al. 2006) and
209 more similar to rates found in other insects (Wilfert et al. 2007). This represents the first
210 estimation of recombination rate in social insects outside of Hymenoptera and
211 demonstrates that eusociality is not a universal driver of high recombination rates.
212 Spearman's correlation between the results from LDhat and LDhelmet, using 10 kbp
213 windows, was $\rho = 0.946$ and $\rho = 0.947$ for *M. bellicosus* and *C. secundus*, respectively, with p
214 $< 2.2 \times 10^{-16}$ for both species. For the remaining analyses, results from the software
215 LDhelmet were used.

216 *Evidence for active recombination hotspots in termite genomes*

217 Recombination rates are highly variable across the genomes of *M. bellicosus* (Figure 2A) and
218 *C. secundus* (Figure 2B). We characterised the distribution of recombination events across
219 the two termite genomes using a cumulative distribution plot (Figure 3). We found that 50%
220 of the recombination occurs in 0.4% of the genome in *M. bellicosus* and 0.2% of the genome
221 in *C. secundus*. This indicates that the majority of recombination events are restricted to a
222 much smaller portion of the genome than observed in *A. mellifera*, where 50% of
223 recombination events occur in 32% of the genome (Wallberg et al. 2015).

224 We further investigated whether recombination hotspots are present in the two termite
225 genomes by looking at the distribution of ρ in windows of 1 kbp, 10 kbp and 100 kbp across
226 the genome (Supplemental Figure S1). For all window sizes, a small subset of windows was
227 observed with ρ greatly exceeding the mean in both termite species. For example, the
228 percentage of 1 kbp windows with recombination rate at least four standard deviations

229 above the genome wide mean value is 0.2% for *M. bellicosus* and 0.6% for *C. secundus*. By
230 contrast, *A. mellifera* has no windows above this limit for any window size, consistent with a
231 lack of recombination hotspots.

232 We next defined hotspots as 2 kbp regions with more than 5-fold higher recombination rate
233 than the surrounding 100 kbp and used STREME (Bailey 2021) to identify 8 to 20-mers that
234 were enriched in hotspots compared to the rest of the genome. This yielded significantly
235 enriched motifs in both species (4 motifs for *M. bellicosus* and 1 motif for *C. secundus* after
236 compensating for multiple hypothesis testing; Supplemental Tables S2 and S3). However,
237 none of the motifs we identified are present in more than 5% of hotspots or exhibit more
238 than 2-fold difference in frequency of occurrence relative to the background, suggesting
239 they are not viable candidate motifs for promoting recombination in hotspots.

240 *Identification and characterization of the PRDM9 gene in termites*

241 We searched the *M. bellicosus* and *C. secundus* genomes for evidence of complete *PRDM9*
242 genes (Figure 4A), which could potentially govern the presence of recombination hotspots in
243 these genomes, as it has been shown to do in mammalian genomes (Myers et al. 2010;
244 Baudat et al. 2010; Parvanov et al. 2010). The *C. secundus* genome contains a *PRDM9*
245 homolog (XP_023708049.2) with annotated KRAB, SSXRD, SET and zinc finger domains
246 (Figure 4B). There is no complete homolog of *PRDM9* in the *M. bellicosus* annotation. We
247 therefore used BLAST to search for sequences homologous to the conserved functional
248 domains from *C. secundus*. We identified a putative *PRDM9* orthologue on Scaffold 42 of the
249 *M. bellicosus* genome assembly, containing all domains in the correct order. We identified
250 retroviral conserved domains in an intron 5' of the zinc-finger domains in this gene, which
251 are not predicted to alter the transcript. We confirmed the presence of a full-length
252 transcript as well as presence and correct order of conserved domains by alignment of the
253 *Zootermopsis nevadensis* *PRDM9* protein sequence to the *M. bellicosus* genome using
254 GeneWise (Madeira et al. 2024)(Figure 4C and Supplemental Table S4).

255 We used a zinc-finger prediction algorithm (Persikov and Singh 2014) to predict DNA binding
256 motifs from the zinc-finger domain present in *PRDM9* in the *M. bellicosus* and *C. secundus*
257 genome assemblies. The most probable consensus motifs were
258 TATGGAACGACAGGAACAACGACATCATCAGCCGCCTAAT and TAATAAGTAGAATCGTTTAG for
259 *M. bellicosus* (Figure 4D) and *C. secundus* (Figure 4E) respectively. Base probability matrices

260 for these motifs are shown in Supplemental Table S5. We tested whether the presence of
261 these motifs corresponded to elevated recombination considering 1 kbp around each motif.
262 However, recombination rate was not significantly elevated around these predicted motifs
263 for either species, either when searching based on the most likely motif, or by searching
264 based on the probability matrices.

265 *Genomic correlates of recombination rate*

266 We analysed genomic correlates of recombination rate in 10 kbp windows. There is a
267 significant correlation between recombination and CpG_{O/E} in both species with Spearman's
268 $\rho = 0.24$, $p < 1 \times 10^{-4}$ for *M. bellicosus* and Spearman's $\rho = 0.10$, $p < 1 \times 10^{-4}$ for *C. secundus*
269 (Supplemental Figure S2). A reduction of recombination rates in regions of low CpG content
270 is consistent with interference of germline methylation with recombination. However, as
271 the correlation coefficients are low, the explanatory power is weak. Correlations of similar
272 magnitudes were observed between recombination and GC content (Spearman's $\rho = 0.23$ for
273 *M. bellicosus*, $p < 1 \times 10^{-4}$ and Spearman's $\rho = 0.017$ for *C. secundus*, $p < 1 \times 10^{-4}$). This
274 correlation has been associated with an effect of recombination in driving GC through GC
275 biased gene conversion but the relatively low correlation coefficients could indicate that this
276 force is not strong in termites. By contrast, the correlation between GC content and
277 recombination rate is much stronger in honey bee ($R^2 = 0.506$), which is likely caused by high
278 recombination rates and intense GC-biased gene conversion (Wallberg et al. 2015).

279 There is a weak but significant correlation between overall repeat element density and
280 recombination rate in *C. secundus* (Spearman's $\rho = 0.02$, $p < 1 \times 10^{-4}$) but not for *M.*
281 *bellicosus*. There is a weak but significant correlation between simple repeats and
282 recombination in both genomes (Spearman's $\rho = 0.051$, $p < 2.22 \times 10^{-16}$ for *M. bellicosus* and
283 Spearman's $\rho = 0.055$, $p < 2.22 \times 10^{-16}$ for *C. secundus*). SINE and LINE elements are also only
284 weakly associated with recombination rate in both genomes (SINEs: Spearman's $\rho = -0.012$,
285 not significant for *M. bellicosus* and Spearman's $\rho = 0.02$, $p < 1 \times 10^{-4}$ for *C. secundus*; LINEs:
286 Spearman's $\rho = -0.02$, $p < 1 \times 10^{-4}$ for *M. bellicosus* and Spearman's $\rho = 0.002$ not significant
287 for *C. secundus*). There is a significant negative correlation between gene density and
288 recombination for the *M. bellicosus* genome (Spearman's $\rho = -0.185$, $p < 2.22 \times 10^{-16}$), but no
289 significant correlation for *C. secundus*. We also tested whether hotspots differ from the

290 background with respect to GC content. The GC content does not differ substantially
291 between hotspots and the rest of the genome in either species (means of 40.1% and 41.0%
292 for *M. bellicosus* and 40.2% and 40.3% for *C. secundus*).

293 We found a significant correlation between nucleotide diversity (π) and recombination in
294 both species (Supplemental Figure S2), with Spearman's $\rho = 0.48$, $p < 1 \times 10^{-4}$ for *M.*
295 *bellicosus* and Spearman's $\rho = 0.31$, $p < 1 \times 10^{-4}$ for *C. secundus*. This correlation is found
296 across a wide range of eukaryotic taxa and is generally accepted to be caused by the
297 interaction between recombination and linked selection (Nachman 2001; Begun and
298 Aquadro 1992).

299 *Recombination and gene expression patterns correlate with CpG_{O/E}*

300 Analysis of the distribution of CpG_{O/E} in both termite species showed that it is bimodally
301 distributed, with substantially lower values in introns and exons compared to flanking
302 noncoding regions (Supplemental Figure S3). This indicates that germline DNA methylation
303 is biased towards gene bodies in the two termite genomes, a pattern that is also found in
304 honey bees and other insect genomes with functional DNA methylation (Harrison et al.
305 2018; Elango et al. 2009; Sarda et al. 2012). We found that exons have lower CpG_{O/E}
306 compared to introns, which are both lower than flanking regions (Figure 5, top row; all
307 comparisons $p < 0.001$ after Bonferroni correction) consistent with higher levels of germline
308 methylation in exons (Supplemental Table S6). We next analysed how recombination rate
309 varies among genomic features. We found that ρ /kbp is also significantly reduced in genes
310 compared to flanking regions for *C. secundus*, with exons also showing reduced ρ /kbp
311 compared to introns (Figure 5, bottom row, all p -values < 0.005 after Bonferroni correction).
312 The same trends are observed in *M. bellicosus* although they are not significant. The
313 correlation between CpG_{O/E} and recombination rate among genes is higher than for the
314 genome overall (Spearman's $\rho = 0.315$, $p < 2.22 \times 10^{-16}$ for *M. bellicosus*; Spearman's $\rho =$
315 0.196 , $p < 2.22 \times 10^{-16}$ for *C. secundus*).

316 We next investigated whether patterns of gene expression between castes and sexes
317 (hereafter, for short 'caste-biased gene expression') were correlated with CpG_{O/E} and
318 recombination rate using gene expression data from two studies (Lin et al. 2021; Elsner et
319 al. 2018). It has been proposed that it is evolutionarily advantageous for genes with worker-

320 biased expression to be located in regions with elevated recombination (Kent et al. 2012).
321 Comparisons of CpG_{O/E} and recombination rate for the original gene expression categories
322 reported by (Elsner et al. 2018) for *M. bellicosus* are shown in Supplemental Figure S4. We
323 also reclassified the genes into the following expression categories: queen-biased, king-
324 biased, worked-biased, male-biased, female-biased, reproduction-biased, and differentially
325 expressed (see methods for details). For *C. secundus*, only worker-biased and queen-biased
326 genes were identified (Lin et al. 2021). We find that mean CpG_{O/E} in gene bodies shows
327 significant variation between gene expression categories in both *M. bellicosus* and *C.*
328 *secundus* (Figure 6). However, this variation is not consistent between species. In *M.*
329 *bellicosus*, queen-biased and female-biased genes have low CpG_{O/E} and king-biased and
330 male-biased genes have high CpG_{O/E}. In *C. secundus*, queen-biased genes have higher than
331 average CpG_{O/E}.

332 The differences in CpG_{O/E} between caste-biased gene expression categories are mirrored by
333 differences in ρ /kbp (Figure 6). Gene expression categories with elevated CpG_{O/E}
334 consistently show elevated ρ /kbp, and this pattern is found in both species. Studies in the
335 honey bee have found that worker-biased genes have lower CpG and higher recombination
336 rates (Kent et al. 2012; Wallberg et al. 2015). In *M. bellicosus*, we find that worker-biased
337 genes have slightly elevated CpG_{O/E} and ρ /kbp. However, in *C. secundus*, these values are
338 reduced in worker-biased genes, whereas queen-biased genes have a slightly elevated
339 CpG_{O/E} and ρ /kbp in this species.

340 We investigated the relative roles of CpG_{O/E} and gene expression in determining ρ in genes
341 using linear models, with CpG_{O/E}, ρ in flanking region and expression categories as
342 explanatory variables. In both *M. bellicosus* and *C. secundus*, we found that CpG_{O/E} was the
343 strongest predictor of recombination rate variation among genes (Supplemental Tables S7
344 and S8) in line with the analyses above. We found that caste-biased expression had no
345 significant impact on the recombination rate. CpG_{O/E} is a better predictor of ρ /kbp in genes
346 than ρ /kbp in flanking region and variation in ρ /kbp among expression categories mainly
347 reflects differences in CpG_{O/E}.

348

349 **Discussion**

350 The main findings we present here are 1) that two distantly related termite species with
351 varying social complexity both have relatively low genomic average rates of meiotic
352 recombination, 2) both genomes possess recombination hotspots and likely contain full-
353 length copies of *PRDM9* and, 3) there are reduced levels of recombination in genomic
354 regions depleted in CpG sites. Our findings contrast with the extremely elevated
355 recombination rates observed in eusocial Hymenoptera, which are likely to be generated by
356 a feature that is specific to these taxa. The finding of recombination hotspots is one of the
357 first in insects. This could reflect a conserved function of *PRDM9* in initiating recombination
358 events in both vertebrates and invertebrates. Our results also support a role for germline
359 methylation in suppressing recombination.

360 *Low recombination rates in termites*

361 Data from a wide range of taxa indicate that at least one crossover per chromosome tetrad
362 is essential for correct chromosomal segregation during meiosis (Fernandes et al. 2018). The
363 chromosome numbers of *M. bellicosus* and *C. secundus* are $2n = 42$ and $2n = 40$, respectively
364 (Jankásek et al. 2021). Considering their assembly lengths, this indicates that a minimum
365 average genomic recombination rate of 0.92 cM/Mb and 1.01 cM/Mb, respectively, would
366 be necessary for accurate meiosis to occur in the two termite species. Our estimates of
367 recombination rate per meiosis based on analysis of LD depend on several factors, including
368 the algorithm to estimate ρ and the estimate of mutation rate. As no estimates of the
369 mutation rate in termites were available, we considered a range of estimates from other
370 insects. These estimates vary by more than an order of magnitude between different insect
371 species (Lynch et al. 2023) and higher estimates of the mutation rate give higher estimates
372 of the recombination rate. Our estimates based on LDhat are all less than 1 cM/Mb for both
373 species, even when considering the highest estimate of mutation rate. Using estimates from
374 LDhelmet and the average of experimentally determined mutation rate estimates in insects
375 gives estimates of recombination rate of 1-2 cM/Mb. The species most closely related to
376 termites for which a mutation rate estimate was available was *H. coronatus* (Huang et al.
377 2023). Using this estimate and ρ from LDhelmet, the recombination rate per meiosis was
378 estimated to 0.57 cM/Mb for *M. bellicosus* and 0.69 cM/Mb for *C. secundus*, i.e. both
379 slightly lower than expected based on the requirement of one crossover per chromosome.
380 Taken together, these results indicate that recombination rates in these two termite species

381 are substantially lower than the elevated values found in eusocial Hymenoptera (6-25
382 cM/Mb) (Wilfert et al. 2007).

383

384 It should be noted that our estimates of recombination rate are sex-averaged rates. It is
385 possible that recombination is absent in one of the termite sexes, which would make a
386 lower sex-averaged recombination rate more feasible. In addition, sex-linked contigs have
387 not been identified in the termite genome assemblies utilized here. *M. bellicosus* and *C.*
388 *secundus* have X1X2/Y1Y2 and X/Y sex-determining systems respectively (Jankásek et al.
389 2021). The inclusion of sex chromosomes in the analysis leads to errors in determining the
390 genome-wide recombination rate per meiosis because they have lower N_E than the rest of
391 the genome. In addition, sex chromosomes are more prone to assembly and read mapping
392 errors, due to reads aligning with the incorrect copy of the chromosome. However,
393 considering that sex chromosomes only comprise a minor portion of the genome, this is
394 unlikely to substantially alter our results. It has also been observed that some chromosomes
395 form ring or chain structures during meiosis in certain termite species (Bergamaschi et al.
396 2007), which could plausibly relax the requirement for one crossover per chromosome per
397 meiosis.

398

399 *Eusociality is not a universal driver of high rates of meiotic recombination*

400 Elevated genomic rates of recombination are characteristic of all eusocial Hymenoptera so
401 far investigated. Several hypotheses have been advanced to explain this phenomenon,
402 which are all based on an evolutionary advantage of recombination in eusocial species
403 (Wilfert et al. 2007). For instance, it has been suggested that elevated recombination could
404 increase genetic diversity in a colony. This could promote diversity in the workforce,
405 enabling more efficient task specialisation among workers (Kent et al. 2012). Alternatively, it
406 could render the colony less susceptible to invasion by parasites and pathogens (Fischer and
407 Schmid-Hempel 2005). Elevated recombination might also favour rapid evolution of caste-
408 specifically expressed genes (Kent and Zayed 2013). In addition, increased recombination
409 could lead to reduced variance in relatedness, which could prevent kin conflict in colonies
410 (Sherman 1979; Templeton 1979).

411 All these hypotheses predict that recombination rate should be elevated in all eusocial
412 insects. Here, however, in the first report of recombination rate in social insects outside of
413 Hymenoptera, we find overall low levels of recombination. Both termite species studied
414 here are eusocial, and in particular *M. bellicosus* has extremely large and complex colonies
415 characteristic of eusociality (Korb and Thorne 2017). The low recombination rate inferred in
416 the two termite genomes prompts re-evaluation of hypotheses connecting eusociality with
417 high recombination rates. Although both termites and social Hymenoptera share many
418 traits, they differ in others that reflect their different ancestries.

419 The chromosome numbers of both termite species (*M. bellicosus*, $2n = 42$; *C. secundus*, $2n =$
420 40) are typical for termites, although variation exists between taxa (Jankásek et al. 2021).
421 These values do not differ from those observed in Hymenoptera, which have a similar range
422 (e.g. *A. mellifera*, $2n = 32$) and do not vary between solitary and eusocial taxa (Cardoso et al.
423 2018; Cunha et al. 2021; Ross et al. 2015). This suggests that differences in chromosome
424 number are unlikely to be relevant in explaining the differences in recombination rates
425 among these taxa.

426 One proposed advantage of sex and recombination is that it is associated with sexual
427 selection and a higher intensity of selection on males. This could be advantageous because
428 differential male mating success can reduce mutational load in sexual populations by
429 causing deleterious mutations to segregate at a lower equilibrium frequency on average
430 (Siller 2001; Agrawal 2001). Recombination is essential for effective purging of deleterious
431 alleles as it unlinks deleterious variants from nearby beneficial ones thus preventing
432 selection interference (Hartfield and Keightley 2012). Selection has been found to be
433 stronger in males than females across animal species (Janicke et al. 2016; Winkler et al.
434 2021). Species with a male-biased sex ratio are expected to experience particularly intense
435 selection on males. It is therefore possible that recombination rate could be particularly
436 elevated in species in which males face intense competition as this increases the
437 evolutionary advantage of recombination.

438 Another proposed advantage of sex and recombination in general is that it is associated
439 with the intensity of sperm competition. Maynard Smith (1976) presented a model that
440 explains how sib-competition can produce an immediate evolutionary advantage to sex and
441 recombination, which occurs when several offspring of a single female compete within a

442 patch. This model was extended by Manning and Chamberlain (1997) who argued that it is
443 analogous to intra-ejaculate competition among sperm, in which recombination increases
444 the variance of fitness. Under these conditions, if inter-ejaculate competition also exists, it is
445 predicted that there will be selection for increased recombination rate. This model predicts
446 a significant correlation between recombination rate and gamete redundancy (excess sperm
447 production), which is observed in mammals (Manning and Chamberlain 1997).

448 Many social Hymenoptera produce highly male-biased reproductive offspring and
449 thousands of haploid male drones compete to fertilise a small number of female queens
450 (Winston 1991; Koeniger et al. 2011; Baer 2005). This situation is similar to sperm
451 competition as haploid males can be considered analogous to gametes. However, as many
452 more genes are expressed in adult haploid males compared to gametes there are more
453 targets of selection. Selection against deleterious alleles is particularly effective in haploid
454 males because recessive deleterious alleles are exposed (Hedrick and Parker 1997). It is
455 therefore possible that the male-biased sex ratio observed in many eusocial Hymenoptera
456 could favour elevated recombination rates in the species so far studied, due to elevated
457 competition between males.

458 Male-biased sex ratios are particularly strong in the genus *Apis*, which is also the genus in
459 which the most extreme recombination rates have been inferred (Beye et al. 2006; Shi et al.
460 2013; Liu et al. 2015; Wallberg et al. 2015; Rueppell et al. 2016; Kawakami et al. 2019).

461 Male-biased sex ratios are also observed in other social bees and wasps. Both male and
462 female biased operational sex ratios have been observed in ants, but are difficult to
463 measure because workers invest more resources in female offspring and may manipulate
464 sex ratios. In non-social Hymenoptera, females lay roughly equal numbers of haploid and
465 diploid eggs (Trivers and Hare 1976). The sex ratio of reproductive males and females is also
466 relatively even in most termite species (Roisin 2001).

467 Further research is needed to determine the cause of variation in recombination rates
468 among social and non-social insects. For example, simulations could be used to determine
469 the effect of selection on haploid males on recombination rates, considering different sex
470 ratios. In addition, it is necessary to estimate recombination rate in a wider range of social
471 and non-social species to determine whether the strength of selection on males is a key
472 factor in determining these rates.

473 *Full length PRDM9 gene and recombination hotspots in termite genomes*

474 Our results are also indicative of the presence of recombination hotspots in the two termite
475 genomes. The fine-scale distribution of recombination rate in both termite genomes shows
476 that 50% of the recombination happens in less than 0.5% of the genome, which is even
477 more extreme than for humans where this corresponds to ~6% of the genome (Myers et al.
478 2005). This contrasts to the honey bee and solitary bees where fine-scale maps are available
479 and recombination is relatively uniformly distributed in the genome (Wallberg et al. 2015;
480 Jones et al. 2019).

481 Two main mechanisms have been shown to lead to recombination hotspots. The first, which
482 is best understood in human and mouse, is governed by the PRDM9 protein. A zinc-finger
483 domain recognises a specific DNA sequence motif and then performs a histone modification
484 in the vicinity, which marks the sequence for a DNA double-stranded break that is repaired
485 by recombination during meiosis (Baudat et al. 2010; Myers et al. 2010; Parvanov et al.
486 2010). In species with this mechanism, both the PRDM9 zinc-finger domain and the
487 sequences present in hotspots are fast evolving, which results in a rapid turnover of hotspot
488 locations (Myers et al. 2010). Full-length PRDM9 orthologues are present among a range of
489 highly-diverged vertebrates including many fish, reptiles and mammals, but many full or
490 partial losses of the gene have also been inferred. In a study of 225 vertebrate genomes, a
491 minimum of six partial and three complete losses were inferred (Baker et al. 2017).
492 However, it is unclear whether PRMD9-hotspots are common in invertebrates.

493 A second mechanism is found in vertebrates that lack PRDM9, in which recombination
494 hotspots are localised to regions of open chromatin such as CpG islands and promoters. This
495 is found in dogs and in most or all birds, in which PRDM9 has been lost, and results in
496 hotspots with stable rather than rapidly evolving locations (Axelsson et al. 2012; Singhal et
497 al. 2015). A similar pattern is also observed in the yeast *Saccharomyces cerevisiae* in which
498 recombination preferentially occurs in promoter regions (Wu and Lichten 1994). PRDM9-
499 independent hotspots can be identified in CpG islands in some vertebrate genomes even
500 when PRDM9 is present (Joseph et al. 2024). In invertebrates such as *Drosophila* and
501 *Caenorhabditis elegans*, recombination hotspots appear to be absent (Coop and Przeworski
502 2007; Chan et al. 2012; Smukowski Heil et al. 2015). In insects, fine-scale maps of social and

503 solitary bees have not revealed recombination hotspots (Wallberg et al. 2015; Jones et al.
504 2019), but there is evidence for hotspots in a butterfly genome (Torres et al. 2023).

505 We find evidence that recombination is directed towards hotspots in both termite species.
506 We also identify a full-length *PRDM9* gene in both species, containing all of the domains
507 needed to initiate recombination. However, we are unable to demonstrate that PRMD9 is
508 responsible for the presence of recombination hotspots in the two genomes. We used a
509 motif prediction algorithm to predict the zinc-finger binding motif in *M. bellicosus* and *C.*
510 *secundus*, but we did not observe elevated recombination rate around instances of the
511 motif in either of the genomes. Furthermore, we did not identify any common sequence
512 motifs that were strongly enriched in recombination hotspots in either of the termite
513 genomes. A plausible interpretation of these observations is that the PRDM9 protein indeed
514 initiates recombination in hotspots in both species, but that positive selection leads to
515 frequent shifts in the target motifs, which results in a lack of a strong association between a
516 specific motif and LD-based hotspots (Myers et al. 2010). It is also possible that the
517 sequences of the zinc-finger motifs are not correctly represented in the genome assemblies,
518 which could result from problems with assembly around minisatellites. However, an
519 unknown mechanism could also be responsible for hotspots in termites.

520 *Evidence that germline DNA methylation suppresses recombination*

521 In insects with a functioning DNA methyltransferase machinery, the CpG_{O/E} statistic shows
522 substantial variation along the genome, which mainly reflects variation in levels of germline
523 DNA methylation (Elango et al. 2009). In contrast to vertebrate genomes, methylation is
524 strongly skewed towards gene bodies in the genomes of insects (Glastad et al. 2011). In the
525 two termite genomes studied here, we find lowest values of CpG_{O/E} in exons, whereas
526 noncoding flanking regions are biased towards higher values, indicative of lower levels of
527 DNA methylation (Figure 5, Supplemental Figure S3). Exons, introns and noncoding flanking
528 regions all display a predominantly bimodal distribution of CpG_{O/E}, likely reflective of the
529 presence of methylated and unmethylated regions. We find that recombination rate is
530 reduced in gene bodies compared to flanking regions in one of the two termite genomes,
531 but the overall genomic correlation between CpG_{O/E} and recombination rate, although
532 significant, is weak. This could reflect the fact that the majority of the genomes are not
533 methylated, so that much of the variation in CpG_{O/E} on the genome scale is not strongly

534 influenced by methylation. Our inference of reduced recombination rates in exons could
535 also be influenced by lower N_E in these regions due to the effects of linked selection, which
536 could result in more extensive LD (Charlesworth 2009). However, the observation that
537 differences in CpG_{O/E} among genes are associated with recombination rate indicates that
538 linked selection is unlikely to be a major factor driving the observed differences in
539 recombination rate and that germline DNA methylation is more important.

540 We identified CpG_{O/E} as the factor with the strongest influence on recombination rate
541 variation among genes. There were no significant effects of differences in gene expression
542 patterns across castes, a result that was also observed in the honey bee genome (Wallberg
543 et al. 2015). This indicates that recombination rate variation is not modulated by differences
544 in gene expression in these genomes, which might be expected if natural selection favours
545 increased recombination rates in certain genes. For example, it has been proposed that
546 natural selection could favour elevated recombination rates in genes with roles in worker
547 behaviour or in immune function due to their important roles in colony function (Wilfert et
548 al. 2007; Kent et al. 2012). However, the results presented here suggest that differences in
549 recombination rate between genes with caste-biased patterns of gene expression are
550 mainly due to underlying differences in methylation levels among genes.

551 A direct effect of germline DNA methylation in suppressing recombination could influence
552 variation in recombination landscapes among vertebrates and invertebrates. Vertebrate
553 genomes are usually highly methylated with the exception of CpG islands. In vertebrate
554 genomes that lack a functional *PRDM9* gene, recombination events tend to localise to CpG
555 islands (for example in dogs and birds) (Singhal et al. 2015; Axelsson et al. 2012). The effect
556 of DNA methylation on recombination rate variation in invertebrates is less clear, but the
557 results presented here also support a role of germline methylation in suppressing
558 recombination.

559

560 **Materials and Methods**

561 *Sample collection*

562 *M. bellicosus* samples were collected from colonies in Kakpin, next to the Comoé National
563 Park in Côte d'Ivoire (coordinates 8°39'N 3°46'W) (Elsner et al. 2018). *C. secundus* colonies

564 were collected from dead *Cerriops tagal* mangrove trees near Palmerston-Channel Island
565 (Darwin Harbor, Northern Territory, Australia; 12°30'S 131°00'E). Colonies were then kept
566 in *Pinus radiata* wood blocks in climate rooms in Germany, providing 28°C, 70% relative
567 humidity, and a 12-h day/night cycle (Lin et al. 2021). For each species, each of the 10
568 collected samples came from a different colony.

569 *Population sequencing*

570 The termites were cut in two, approximately between head and thorax. DNA was extracted
571 from both parts using the QIAGEN Blood and Tissue Kit following the standard protocol,
572 including treatment with 4 µL RNase and 25 µL Proteinase K. The DNA extraction product
573 was cleaned and concentrated with ZymoResearch Genomic DNA Clean & Concentrator kit.
574 For most samples, the RNase treatment was repeated prior to cleaning and concentrating.
575 One DNA sample from each individual was chosen, based on the DNA amount and quality,
576 to be sequenced. Sequencing libraries were produced using the Illumina DNA PCR-free
577 library preparation kit according to the manufacturers protocol, using an input DNA quantity
578 of 200 ng per sample. This protocol yields insert sizes of approximately 350 bp. We
579 performed Illumina short-read sequencing on the libraries using NovaSeq 6000 S4 flow cell
580 with 2 x 150 bp paired end reads.

581 *Read mapping and variant calling*

582 The sequence data from the two termite species were mapped to the reference genomes
583 for *M. bellicosus* (Qiu et al. 2023) and *C. secundus* (Csec_1.0) (Harrison et al. 2018)
584 respectively, using Burrows-Wheeler alignment tool BWA version 0.7.17 (Li & Durbin 2009)
585 with the BWA-MEM algorithm. Sorting and indexing of the BAM-files was done with the
586 SAMtools package version 1.17 (Li et al. 2009), followed by adding read groups and marking
587 duplicate reads with Picard toolkit version 1.118 (<http://broadinstitute.github.io/picard/>).
588 After mapping, we excluded all scaffolds < 1 kbp from the *C. secundus* genome, which in
589 total correspond to 2% of the genome size, as they are potentially of lower quality and not
590 informative for analysis of linkage disequilibrium or recombination. For *M. bellicosus* there
591 are no scaffolds shorter than 1 kbp, but we excluded the following five scaffolds, which
592 together correspond to 3.78% of the genome length, due to unexpectedly high
593 heterozygosity: 93, 62, 41, 35 and 32.

594 One of the *C. secundus* individuals did not map well to the reference genome (71% mapped
595 reads, unequal distribution between forward and reverse strand and an average mapping
596 quality of 35 while all the other samples had an average mapping quality >45). This
597 individual was excluded from all further analyses and hence the total number of termite
598 individuals analysed in this study is 19, including 10 *M. bellicosus* and 9 *C. secundus*.

599 Variant calling was done using the tools HaplotypeCaller, GenomicsDBImport and
600 GenotypeGVCFs from GATK version 4.3.0.0 as described in their best practices workflow
601 ([https://gatk.broadinstitute.org/hc/en-us/articles/360035535932-Germline-short-variant-](https://gatk.broadinstitute.org/hc/en-us/articles/360035535932-Germline-short-variant-discovery-SNPs-Indels-)
602 [discovery-SNPs-Indels-](https://gatk.broadinstitute.org/hc/en-us/articles/360035535932-Germline-short-variant-discovery-SNPs-Indels-), last accessed 2023-07-11). The variants were filtered in multiple
603 steps, first removing extended regions of low mapping quality or deviating read depth as
604 those regions are likely to be unreliable. This was done based on statistics from the
605 SAMtools mpileup and depth tools, respectively, removing 100 kbp windows with mean
606 mapping quality below 70 or mean read depth more than two standard deviations from the
607 genome-wide mean. Indels were removed using VCFtools version 0.1.16 (Danecek et al.
608 2011) before GATK VariantFiltration was run with the following limits, which are all equal to
609 or stricter than the ones recommended ([https://gatk.broadinstitute.org/hc/en-](https://gatk.broadinstitute.org/hc/en-us/articles/360035890471-Hard-filtering-germline-short-variants)
610 [us/articles/360035890471-Hard-filtering-germline-short-variants](https://gatk.broadinstitute.org/hc/en-us/articles/360035890471-Hard-filtering-germline-short-variants), last accessed 2023-07-11)
611 and adapted to the observed distributions of the corresponding statistics: QD<2; FS>50;
612 MQ<40; ReadPosRankSum< -4; ReadPosRankSum>4; SOR>3; ExcessHet>5 for both species
613 as well as MQRankSum with limits -5 and 5 for *C. secundus* and limits -6 and 4 for *M.*
614 *bellicosus*. This was followed by additional filtering with VCFtools to select only bi-allelic
615 sites with a minimum quality score of 30 and maximum of 40% missing genotypes. The SNPs
616 with mean read depth in the lowest or highest 2.5% of the depth distribution were also
617 filtered out, which translates to a depth below 10 or above 34 for *C. secundus* and below 5
618 or above 40 for *M. bellicosus*. For the recombination rate calculations, the SNPs were also
619 filtered for a minor allele count ≥ 2 , as rare variants appearing on only one chromosome
620 have a relatively high false positive rate and are not informative regarding LD. The average
621 proportion of missing genotypes per individual was 4.5×10^{-5} for *C. secundus* and 1.2×10^{-4}
622 for *M. bellicosus*. After variant calling and filtering, the data was phased and imputed using
623 Beagle version 5.1 (Browning and Browning 2007; Browning et al. 2018).

624 *Estimation of LD decay*

625 The decay of linkage disequilibrium, r^2 , with increasing physical distance was estimated with
626 the software PopLDDecay version 3.42 (Zhang et al. 2019) over a maximum distance of 10
627 kbp. For this analysis, sequence data from *A. mellifera scutellata* was included for
628 comparison (Wallberg et al. 2017). The *A. m. scutellata* sequences were mapped to the
629 Amel_HAv3.1 reference genome (Wallberg et al. 2019) and processed and filtered in the
630 same way as described above for the termite data (GATK VariantFiltration with the limits
631 $QD < 2$, $FS > 25$, $MQ < 40$, $MQRankSum < -4$, $MQRankSum > 4$, $ReadPosRankSum < -4$,
632 $ReadPosRankSum > 4$, $SOR > 3$, $ExcessHet > 5$ and VCFtools to select bi-allelic sites with mean
633 read depth between 5-13, quality score ≥ 30 , minor allele count ≥ 2 and $\leq 40\%$ missing
634 genotypes). For *M. bellicosus*, the reference genome contains some gaps of unknown size
635 and in order to avoid estimating r^2 across those gaps, scaffold breaks were introduced at the
636 corresponding positions.

637 *Estimation of population recombination rate*

638 We estimated the population-scaled recombination rate, ρ , using two methods: LDhat
639 (Auton and McVean 2007) and LDhelmet (Chan et al. 2012), which are both based on a
640 Bayesian reversible-jump Markov Chain Monte Carlo algorithm (rjMCMC).

641 For LDhat (<https://github.com/auton1/Ldhat>, downloaded 2023-04-19), the input files were
642 generated from the filtered vcf-file with VCFtools and the `--ldhat` option. Then the LDhat
643 function complete was run in order to create a lookup table, with the estimated value of θ_w
644 (see below), a maximum ρ value of 100 and 101 grid points, as recommended. This was
645 followed by the main function, interval, to perform the rjMCMC with 10 million iterations,
646 sampling every 5000th iteration and a block penalty of 1 as this has been used previously
647 with LDhat in similar studies (Wallberg et al. 2015; Jones et al. 2019). In order to summarise
648 the output from interval, the stat function was used, discarding the first 20 samples as burn-
649 in.

650 The recombination rate was also estimated using the software LDhelmet version 1.10 (Chan
651 et al. 2012). In order to prepare the input files for LDhelmet, the filtered vcf-files were
652 converted into multiple-sequence fasta-files using the vcf2fasta function from vcflib version
653 2017-04-04 (Garrison et al. 2022) and to the related file formats .snps and .pos with the `--`
654 `ldhelmet` option from VCFtools (version 0.1.16). The first step of the LDhelmet workflow is

655 to create haplotype configuration files with the `find_confs` tool, followed by generation of
656 likelihood lookup tables with the tool `table_gen` and computation of Padé coefficients with
657 the tool `pade`. These tools were run with the recommended parameters, meaning that
658 `find_confs` was run with a window size of 50 SNPs, `table_gen` was run with a grid of ρ -values
659 ranging from 0 to 100 with increments of 0.1 up to 10 and increments of 1 for the remaining
660 grid and `pade` was run to generate 11 Padé coefficients. Scaffolds shorter than or equal to
661 the window size of 50 SNPs were removed, corresponding to 1% of the sequence length in
662 *C. secundus* and even less for *M. bellicosus*. The tool `rjmcmmc` which contains the main
663 algorithm was run with a burn-in of 100,000 followed by 1,000,000 iterations with a block
664 penalty of 50 as recommended (Chan et al. 2012). For each species, the `rjmcmmc` tool was run
665 three times with different seeds and the convergence between the replicates was evaluated
666 in terms of Spearman's rank correlation coefficient, which was > 0.95 with $p < 2.2 \times 10^{-16}$ for
667 all pairwise comparisons of both species. The binary output from `rjmcmmc` was converted to
668 text, extracting the mean ρ -value between each pair of SNPs, using the tool `post_to_text`.

669 The outputs from `LDhat` and `LDhelmet` give the value of the parameter ρ between each pair
670 of consecutive SNPs. Those values were converted to equally sized windows across each
671 scaffold, as well as the coordinates of individual genomic features, by taking a weighted
672 average of values from overlapping intervals. The *M. bellicosus* scaffolds contain a few gaps
673 of unknown size and the values between SNPs across such gaps were removed.

674 The parameter ρ is proportional to the recombination rate r and the effective population
675 size N_E , which in turn can be estimated based on the mutation rate μ and the number of
676 segregating sites, K . In order to convert ρ to r , the following equations were used, where n is
677 the number of haploid sequences. The number of segregating sites (K) was calculated before
678 the filter on minor allele count ≥ 2 was applied, as this filter likely removes many true SNPs
679 as well, which could affect the estimates.

680 θ_W was estimated for each sample using the equation below from (Watterson 1975):

$$\theta_W = K / \sum_{i=1}^{n-1} \frac{1}{i}$$

681 We used the value of θ_W to estimate N_E using:

$$N_E = \frac{\theta_W}{4\mu}$$

682 We estimated N_E using a range of mutation rates estimated from other insect species
 683 (Keightley et al. 2009, 2014, 2015; Yang et al. 2015; Liu et al. 2017; Lynch et al. 2023). We
 684 then estimated the recombination rate using the following equation, assuming a range of
 685 values of N_E .

$$r = \frac{\rho}{4N_E}$$

686

687 *Cumulative plot of rho ρ /kbp*

688 A cumulative plot of the proportion of recombination events versus the proportion of the
 689 physical distance along the genome was constructed based on estimates of ρ /bp for the two
 690 termite species and previous estimates for *A. mellifera* (Wallberg et al. 2015; PRJNA236426).
 691 The ρ /bp estimates between markers were placed in decreasing order before multiplication
 692 with the respective physical distances between the markers. Then cumulative sums were
 693 calculated for the ρ -values as well as the corresponding physical distances and divided by
 694 the total genome-wide sums.

695 *k-mer enrichment in recombination hotspots*

696 In order to identify k -mers associated with elevated recombination rate, we defined
 697 recombination hotspots as 2 kbp segments with at least five-fold elevated recombination
 698 rate compared to the local background, as defined by 50 kbp flanking up and downstream of
 699 the segment, resulting in 39837 regions for *M. bellicosus* and 40894 regions for *C. secundus*.

700 Then, we used these hotspots to search for motifs associated with elevated recombination
 701 rate by comparing against an equivalent number of randomly chosen 2 kbp regions from the
 702 rest of the genome. This was done using STREME 5.5.4 (Bailey 2021) using a minimum and
 703 maximum size of k -mer of 8 and 20, (`--minw 8 ; --maxw 20`) and otherwise default options.
 704 From all motifs with significant enrichment after adjusting for multiple testing, we then
 705 considered only motifs present in more than 5% of all hotspots and an at least two-fold
 706 enrichment compared to the background as credible candidates.

707 *Identifying PRDM9 orthologues in M. bellicosus and C. secundus*

708 A full-length copy of PRDM9 is present in the *C. secundus* genome annotation, but not in *M.*
709 *bellicosus*. Using OrthoFinder (Emms and Kelly 2019), and the genome annotation files for
710 both species, we identified a single orthologue to the *C. secundus* PRDM9 in *M. bellicosus*.
711 We analysed this region using the NCBI conserved domain search (Wang et al. 2023). We
712 also searched the *M. bellicosus* assembly for the PR/SET domains derived from *C. secundus*
713 and *Zootermopsis nevadensis* using BLAST (Camacho et al. 2009) and subsequently for all
714 other PRDM9 domains (KRAB, SSXRD, ZF-Casette) to identify hits that contain all other
715 PRDM9 domains in the vicinity in the correct order. We used GeneWise (Madeira et al.
716 2024) with default options to perform gapped alignment of a the PRDM9 protein sequence
717 from *Zootermopsis nevadensis* against the target region to predict exon-intron borders.

718 *Predicting binding sites from zinc-finger-motifs*

719 Using the ZF-motifs from *C. secundus*, we obtained letter probability matrices for predicted
720 binding motifs using a webserver (<http://zf.princeton.edu/index.php> ; (Persikov and Singh
721 2014) which were used to search for binding sites across the genome using FIMO (Grant et
722 al. 2011) with default options. Subsequently, the mean rho for the surrounding 1 kbp bin
723 was used to test for a difference in mean rho between bins associated with a suspected
724 binding site, and a similar number of randomly chosen bins without association. For
725 significance testing, we repeated this draw 10.000 times to compare the associated bins
726 against the 95% confidence interval of the resulting distribution.

727 *Analysis of genomic correlates of recombination*

728 We divided the genome into 10 kbp windows in which average ρ and other genomic
729 features were estimated. Windows shorter than 5 kbp (half of the specified window size),
730 which appear in short scaffolds or at the ends at longer scaffolds, were excluded from the
731 analyses (excluding less than 1% of the sequence for each species). Correlation coefficients
732 were estimated with Spearman's ρ , with significance estimated by permutation tests with
733 10,000 iterations.

734 In order to determine the repeat content across the *M. bellicosus* and *C. secundus* genome
735 assemblies, we first generated custom repeat libraries for each species with RepeatModeler
736 (Flynn et al. 2020) using default options. This was then combined with Repbase 29 (Bao et
737 al. 2015) and Dfam 3.8 (Storer et al. 2021) and used to run RepeatMasker with default

738 options on each genome. We estimated the proportion of sequence in each repeat class in
739 10 kbp windows and used Spearman's rank correlation to correlate this with estimates of
740 recombination rate.

741 *Per gene recombination rate and CpG_{O/E} ratio*

742 The observed/expected frequency of CpG sites (CpG_{O/E}) and mean ρ were calculated on a
743 per-gene basis, as well as for exons and introns, and 50 kbp flanking regions 10 kbp
744 upstream and downstream of the gene, akin to Wallberg et al (2015). For recombination
745 rate, estimates of ρ between markers were used, utilising a weighted mean when the
746 element spanned multiple markers. For visualisation, extreme CpG_{O/E} values due to low GC
747 content were set to a maximum of 4.

748 We tested for significant difference in mean between ρ and CpG_{O/E} in flanking regions, exons
749 and introns using paired *t*-tests corrected for multiple testing using a Bonferroni threshold.

750 *Differential expression data*

751 We classified genes in both species according to their caste-biased patterns of expression
752 from two studies (Elsner et al. 2018; Lin et al. 2021). Elsner et al. (2018) analysed four castes
753 of *M. bellicosus*, with two age classes of each: major and minor workers, queens and kings.
754 They analysed differences in gene expression among these classes using RNA-seq data. We
755 reclassified the differential expression data by grouping the direct caste-vs-caste
756 comparisons as "queen-biased", "king-biased", "worker-biased", "reproduction-biased",
757 "male-biased" or "female-biased" if they were differentially upregulated for this caste (or
758 group) in comparison to other castes (or groups). Since Elser *et al.* (2018) initially mapped
759 the *M. bellicosus* reads against the *Macrotermes natalensis* genome, We used OrthoFinder
760 (Emms and Kelly 2019) to identify the *M. bellicosus* orthologues corresponding to the
761 differentially expressed genes. Only single-copy genes were considered for this analysis.

762 Lin et al. (2021), performed RNA-seq on samples of workers and queens. Here, we used the
763 data from untreated queens and workers. Differentially expressed *C. secundus* genes were
764 classified as "worker-biased" or "queen-biased" if they were differentially expressed with a
765 bias to the respective caste, or unbiased if they were not, and subsequently compared
766 between classes. The lists of genes we identified in the caste-biased categories in both
767 species are provided as Supplemental Tables S9 and S10.

768 *Correlates of recombination rate variation among genes*

769 In order to assess the relative importance of CpG_{O/E} and differential expression patterns on
770 recombination rate in genes (genic ρ /kbp), two ordinary least squares models were built
771 using statsmodels (Seabold and Perktold 2010) for each termite species. Genic CpG_{O/E},
772 differential expression categories and flanking region ρ /kbp were used as exogenous
773 variables. In the first model, we included flanking region ρ /kbp and CpG_{O/E}. In the second
774 model, we included all available biased expression categories for each species.

775

776 **Data access**

777 The Illumina whole-genome sequencing data generated in this study have been submitted
778 to the NCBI BioProject database (<https://www.ncbi.nlm.nih.gov/bioproject/>) under
779 accession number PRJNA1021607. Custom scripts are available on GitHub
780 (<https://github.com/troe27/termite-recombination-rate>) and as Supplemental Code.

781

782 **Competing interest statement**

783 The authors declare no competing interests.

784

785 **Acknowledgements**

786 We acknowledge grant 2018-03896 from The Swedish Research Council to MTW and from
787 the Deutsche Forschungsgemeinschaft (DFG) KO-1895/26-1: 417980976 to JK. We
788 acknowledge support from the National Genomics Infrastructure in Stockholm funded by
789 Science for Life Laboratory, the Knut and Alice Wallenberg Foundation and the Swedish
790 Research Council. The computations were enabled by resources in project NAISS 2023/23-
791 402 provided by the National Academic Infrastructure for Supercomputing in Sweden
792 (NAISS) at UPPMAX, funded by the Swedish Research Council through grant agreement no.
793 2022-06725. We thank Göran Arnqvist for helpful discussions on the evolution of sex and
794 recombination and Marie Raynaud for assistance running LDhelmet. The Parks and Wildlife
795 Commission, Northern Territory, and the Department of the Environment, Water, Heritage
796 and the Arts, Australia, gave permission to collect (Permit number 59044) and export

797 (PWS2016-001559) the *C. secundus* termites. The Office Ivoirien des Parcs et Réserves
798 (OIPR) provided sampling and export permits for the *M. bellicosus* samples. The study was
799 conducted according to the Nagoya protocol. MTW designed and led the research; TE and
800 TR conducted the analysis; MTW, TE, TR and JK wrote the paper; DE and JK contributed data
801 and samples; AO, YL, and TL performed lab work.

802

803 **References**

- 804 Agrawal AF. 2001. Sexual selection and the maintenance of sexual reproduction. *Nature*
805 **411**: 692–695.
- 806 Arsala D, Wu X, Yi SV, Lynch JA. 2022. Dnmt1a is essential for gene body methylation and
807 the regulation of the zygotic genome in a wasp. *PLOS Genetics* **18**: e1010181.
- 808 Auton A, McVean G. 2007. Recombination rate estimation in the presence of hotspots.
809 *Genome Research* **17**: 1219–27.
- 810 Axelsson E, Webster MT, Ratnakumar A, Consortium L, Ponting CP, Lindblad-Toh K. 2012.
811 Death of PRDM9 coincides with stabilization of the recombination landscape in the
812 dog genome. *Genome Res* **22**: 51–63.
- 813 Baer B. 2005. Sexual selection in Apis bees. *Apidologie* **36**: 187–200.
- 814 Bailey TL. 2021. STREME: accurate and versatile sequence motif discovery. *Bioinformatics*
815 **37**: 2834–2840.
- 816 Baker Z, Schumer M, Haba Y, Bashkirova L, Holland C, Rosenthal GG, Przeworski M. 2017.
817 Repeated losses of PRDM9-directed recombination despite the conservation of
818 PRDM9 across vertebrates ed. B. De Massy. *eLife* **6**: e24133.
- 819 Bao W, Kojima KK, Kohany O. 2015. Repbase Update, a database of repetitive elements in
820 eukaryotic genomes. *Mobile DNA* **6**: 11.
- 821 Baudat F, Buard J, Grey C, Fledel-Alon A, Ober C, Przeworski M, Coop G, de Massy B. 2010.
822 PRDM9 is a major determinant of meiotic recombination hotspots in humans and
823 mice. *Science* **327**: 836–840.
- 824 Begun DJ, Aquadro CF. 1992. Levels of naturally occurring DNA polymorphism correlate with
825 recombination rates in *D. melanogaster*. *Nature* **356**: 519–520.
- 826 Bergamaschi S, Dawes-Gromadzki TZ, Scali V, Marini M, Mantovani B. 2007. Karyology,
827 mitochondrial DNA and the phylogeny of Australian termites. *Chromosome Res* **15**:
828 735–753.

- 829 Berglund J, Quilez J, Arndt PF, Webster MT. 2014. Germline methylation patterns determine
830 the distribution of recombination events in the dog genome. *Genome Biol Evol* **7**:
831 522–530.
- 832 Bewick AJ, Sanchez Z, Mckinney EC, Moore AJ, Moore PJ, Schmitz RJ. 2019. Dnmt1 is
833 essential for egg production and embryo viability in the large milkweed bug,
834 *Oncopeltus fasciatus*. *Epigenetics & Chromatin* **12**: 6.
- 835 Beye M, Gattermeier I, Hasselmann M, Gempe T, Schioett M, Baines JF, Schlipalius D,
836 Mougel F, Emore C, Rueppell O, et al. 2006. Exceptionally high levels of
837 recombination across the honey bee genome. *Genome research* **16**: 1339–44.
- 838 Browning BL, Zhou Y, Browning SR. 2018. A One-Penny Imputed Genome from Next-
839 Generation Reference Panels. *The American Journal of Human Genetics* **103**: 338–
840 348.
- 841 Browning SR, Browning BL. 2007. Rapid and accurate haplotype phasing and missing-data
842 inference for whole-genome association studies by use of localized haplotype
843 clustering. *Am J Hum Genet* **81**: 1084–1097.
- 844 Camacho C, Coulouris G, Avagyan V, Ma N, Papadopoulos J, Bealer K, Madden TL. 2009.
845 BLAST+: architecture and applications. *BMC Bioinformatics* **10**: 421.
- 846 Cardoso DC, Santos HG, Cristiano MP. 2018. The Ant Chromosome database – ACdb: an
847 online resource for ant (Hymenoptera: Formicidae) chromosome researchers.
848 *Myrmecological News* **27**: 87–91.
- 849 Chan AH, Jenkins PA, Song YS. 2012. Genome-Wide Fine-Scale Recombination Rate Variation
850 in *Drosophila melanogaster*. *PLOS Genetics* **8**: e1003090.
- 851 Charlesworth B. 2009. Fundamental concepts in genetics: effective population size and
852 patterns of molecular evolution and variation. *Nat Rev Genet* **10**: 195–205.
- 853 Coop G, Przeworski M. 2007. An evolutionary view of human recombination. *Nature reviews*
854 *Genetics* **8**: 23–34.
- 855 Cunha MS, Cardoso DC, Cristiano MP, de Oliveira Campos LA, Lopes DM. 2021. The Bee
856 Chromosome database (Hymenoptera: Apidae). *Apidologie* **52**: 493–502.
- 857 Elango N, Hunt BG, Goodisman MA, Yi SV. 2009. DNA methylation is widespread and
858 associated with differential gene expression in castes of the honeybee, *Apis*
859 *mellifera*. *Proceedings of the National Academy of Sciences of the United States of*
860 *America* **106**: 11206–11.
- 861 Elsner D, Meusemann K, Korb J. 2018. Longevity and transposon defense, the case of
862 termite reproductives. *PNAS* **115**: 5504–5509.
- 863 Emms DM, Kelly S. 2019. OrthoFinder: phylogenetic orthology inference for comparative
864 genomics. *Genome Biology* **20**: 238.

- 865 Fazalova V, Nevado B. 2020. Low Spontaneous Mutation Rate and Pleistocene Radiation of
866 Pea Aphids. *Mol Biol Evol* **37**: 2045–2051.
- 867 Fernandes JB, Séguéla-Arnaud M, Larchevêque C, Lloyd AH, Mercier R. 2018. Unleashing
868 meiotic crossovers in hybrid plants. *Proceedings of the National Academy of Sciences*
869 **115**: 2431–2436.
- 870 Fischer O, Schmid-Hempel P. 2005. Selection by parasites may increase host recombination
871 frequency. *Biol Lett* **1**: 193–195.
- 872 Flynn JM, Hubley R, Goubert C, Rosen J, Clark AG, Feschotte C, Smit AF. 2020.
873 RepeatModeler2 for automated genomic discovery of transposable element families.
874 *Proceedings of the National Academy of Sciences* **117**: 9451–9457.
- 875 Garrison E, Kronenberg ZN, Dawson ET, Pedersen BS, Prins P. 2022. A spectrum of free
876 software tools for processing the VCF variant call format: vcflib, bio-vcf, cyvcf2, hts-
877 nim and slivar. *PLOS Computational Biology* **18**: e1009123.
- 878 Glastad KM, Hunt BG, Yi SV, Goodisman M a. D. 2011. DNA methylation in insects: on the
879 brink of the epigenomic era. *Insect Molecular Biology* **20**: 553–565.
- 880 Grant CE, Bailey TL, Noble WS. 2011. FIMO: scanning for occurrences of a given motif.
881 *Bioinformatics* **27**: 1017–1018.
- 882 Harrison MC, Jongepier E, Robertson HM, Arning N, Bitard-Feildel T, Chao H, Childers CP,
883 Dinh H, Doddapaneni H, Dugan S, et al. 2018. Hemimetabolous genomes reveal
884 molecular basis of termite eusociality. *Nature Ecology & Evolution* **2**: 557–566.
- 885 Hartfield M, Keightley PD. 2012. Current hypotheses for the evolution of sex and
886 recombination. *Integrative Zoology* **7**: 192–209.
- 887 Hedrick PW, Parker JD. 1997. Evolutionary Genetics and Genetic Variation of Haplodiploids
888 and X-Linked Genes. *Annual Review of Ecology and Systematics* **28**: 55–83.
- 889 Hoffmann K, Foster KR, Korb J. 2012. Nest value mediates reproductive decision making
890 within termite societies. *Behavioral Ecology* **23**: 1203–1208.
- 891 Huang G, Song L, Du X, Huang X, Wei F. 2023. Evolutionary genomics of camouflage
892 innovation in the orchid mantis. *Nat Commun* **14**: 4821.
- 893 Janicke T, Häderer IK, Lajeunesse MJ, Anthes N. 2016. Darwinian sex roles confirmed across
894 the animal kingdom. *Science Advances* **2**: e1500983.
- 895 Jankásek M, Kotyková Varadínová Z, Šťáhlavský F. 2021. Blattodea Karyotype Database. *EJE*
896 **118**: 192–199.
- 897 Jones JC, Wallberg A, Christmas MJ, Kapheim KM, Webster MT. 2019. Extreme Differences in
898 Recombination Rate between the Genomes of a Solitary and a Social Bee. *Mol Biol*
899 *Evol* **36**: 2277–2291.

- 900 Joseph J, Prentout D, Laverré A, Tricou T, Duret L. 2024. High prevalence of PRDM9-
901 independent recombination hotspots in placental mammals. *Proceedings of the*
902 *National Academy of Sciences* **121**: e2401973121.
- 903 Kawakami T, Wallberg A, Olsson A, Wintermantel D, de Miranda JR, Allsopp M, Rundlöf M,
904 Webster MT. 2019. Substantial Heritable Variation in Recombination Rate on
905 Multiple Scales in Honeybees and Bumblebees. *Genetics* **212**: 1101–1119.
- 906 Keightley PD, Ness RW, Halligan DL, Haddrill PR. 2014. Estimation of the Spontaneous
907 Mutation Rate per Nucleotide Site in a *Drosophila melanogaster* Full-Sib Family.
908 *Genetics* **196**: 313–320.
- 909 Keightley PD, Pinharanda A, Ness RW, Simpson F, Dasmahapatra KK, Mallet J, Davey JW,
910 Jiggins CD. 2015. Estimation of the Spontaneous Mutation Rate in *Heliconius*
911 *melpomene*. *Mol Biol Evol* **32**: 239–243.
- 912 Keightley PD, Trivedi U, Thomson M, Oliver F, Kumar S, Blaxter ML. 2009. Analysis of the
913 genome sequences of three *Drosophila melanogaster* spontaneous mutation
914 accumulation lines. *Genome Res* **19**: 1195–1201.
- 915 Kent CF, Minaei S, Harpur BA, Zayed A. 2012. Recombination is associated with the
916 evolution of genome structure and worker behavior in honey bees. *PNAS* **109**:
917 18012–18017.
- 918 Kent CF, Zayed A. 2013. Evolution of recombination and genome structure in eusocial
919 insects. *Communicative & Integrative Biology* **6**: e22919.
- 920 Koeniger G, Koeniger N, Phiancharoen M. 2011. Comparative Reproductive Biology of
921 Honeybees. In *Honeybees of Asia* (eds. H.R. Hepburn and S.E. Radloff), pp. 159–206,
922 Springer, Berlin, Heidelberg https://doi.org/10.1007/978-3-642-16422-4_8 (Accessed
923 February 13, 2024).
- 924 Korb J. 2008. Termites, hemimetabolous diploid white ants? *Frontiers in Zoology* **5**: 15.
- 925 Korb J, Hartfelder K. 2008. Life history and development - a framework for understanding
926 developmental plasticity in lower termites. *Biological Reviews* **83**: 295–313.
- 927 Korb J, Thorne B. 2017. Sociality in Termites. In *Comparative Social Evolution* (eds. D.R.
928 Rubenstein and P. Abbot), pp. 124–153, Cambridge University Press, Cambridge
929 [https://www.cambridge.org/core/books/comparative-social-evolution/sociality-in-](https://www.cambridge.org/core/books/comparative-social-evolution/sociality-in-termites/11A80CB9FA947760889676E03899E85C)
930 [termites/11A80CB9FA947760889676E03899E85C](https://www.cambridge.org/core/books/comparative-social-evolution/sociality-in-termites/11A80CB9FA947760889676E03899E85C) (Accessed August 9, 2023).
- 931 Krasovec M. 2021. The spontaneous mutation rate of *Drosophila pseudoobscura*. *G3*
932 (*Bethesda*) **11**: jkab151.
- 933 Lam I, Keeney S. 2015. Nonparadoxical evolutionary stability of the recombination initiation
934 landscape in yeast. *Science* **350**: 932–937.

- 935 Leffler EM, Bullaughey K, Matute DR, Meyer WK, Ségurel L, Venkat A, Andolfatto P,
936 Przeworski M. 2012. Revisiting an Old Riddle: What Determines Genetic Diversity
937 Levels within Species? *PLoS Biol* **10**: e1001388.
- 938 Lin S, Werle J, Korb J. 2021. Transcriptomic analyses of the termite, *Cryptotermes secundus*,
939 reveal a gene network underlying a long lifespan and high fecundity. *Commun Biol* **4**:
940 1–12.
- 941 Liu H, Jia Y, Sun X, Tian D, Hurst LD, Yang S. 2017. Direct Determination of the Mutation Rate
942 in the Bumblebee Reveals Evidence for Weak Recombination-Associated Mutation
943 and an Approximate Rate Constancy in Insects. *Mol Biol Evol* **34**: 119–130.
- 944 Liu H, Zhang X, Huang J, Chen J-Q, Tian D, Hurst LD, Yang S. 2015. Causes and consequences
945 of crossing-over evidenced via a high-resolution recombinational landscape of the
946 honey bee. *Genome Biol* **16**: 15.
- 947 Lyko F, Foret S, Kucharski R, Wolf S, Falckenhayn C, Maleszka R. 2010. The Honey Bee
948 Epigenomes: Differential Methylation of Brain DNA in Queens and Workers. *PLoS*
949 *Biol* **8**: e1000506.
- 950 Lynch M, Ali F, Lin T, Wang Y, Ni J, Long H. 2023. The divergence of mutation rates and
951 spectra across the Tree of Life. *EMBO reports* **24**: e57561.
- 952 Madeira F, Madhusoodanan N, Lee J, Eusebi A, Niewielska A, Tivey ARN, Lopez R, Butcher S.
953 2024. The EMBL-EBI Job Dispatcher sequence analysis tools framework in 2024.
954 *Nucleic Acids Research* gkae241.
- 955 Manning JT, Chamberlain AT. 1997. Sib competition and sperm competitiveness: an answer
956 to ‘Why so many sperms?’ and the recombination/sperm number correlation.
957 *Proceedings of the Royal Society of London Series B: Biological Sciences* **256**: 177–
958 182.
- 959 Maynard Smith J. 1976. A short-term advantage for sex and recombination through sib-
960 competition. *Journal of Theoretical Biology* **63**: 245–258.
- 961 Misof B, Liu S, Meusemann K, Peters RS, Donath A, Mayer C, Frandsen PB, Ware J, Flouri T,
962 Beutel RG, et al. 2014. Phylogenomics resolves the timing and pattern of insect
963 evolution. *Science* **346**: 763–767.
- 964 Myers S, Bottolo L, Freeman C, McVean G, Donnelly P. 2005. A fine-scale map of
965 recombination rates and hotspots across the human genome. *Science* **310**: 321–4.
- 966 Myers S, Bowden R, Tumian A, Bontrop RE, Freeman C, Macfie TS, McVean G, Donnelly P.
967 2010. Drive against hotspot motifs in primates implicates the PRDM9 gene in meiotic
968 recombination. *Science* **327**: 876–9.
- 969 Nachman MW. 2001. Single nucleotide polymorphisms and recombination rate in humans.
970 *Trends in genetics*: *TIG* **17**: 481–5.

- 971 Niehuis O, Gibson JD, Rosenberg MS, Pannebakker BA, Koevoets T, Judson AK, Desjardins
972 CA, Kennedy K, Duggan D, Beukeboom LW, et al. 2010. Recombination and Its Impact
973 on the Genome of the Haplodiploid Parasitoid Wasp *Nasonia*. *PLOS ONE* **5**: e8597.
- 974 Parvanov ED, Petkov PM, Paigen K. 2010. Prdm9 controls activation of mammalian
975 recombination hotspots. *Science* **327**: 835–835.
- 976 Persikov AV, Singh M. 2014. De novo prediction of DNA-binding specificities for Cys2His2
977 zinc finger proteins. *Nucleic Acids Research* **42**: 97–108.
- 978 Qiu B, Elsner D, Korb J. 2023. High-quality long-read genome assemblies reveal evolutionary
979 patterns of transposable elements and DNA methylation in termites.
980 2023.10.31.564968.
981 <https://www.biorxiv.org/content/10.1101/2023.10.31.564968v1> (Accessed January
982 8, 2024).
- 983 Roisin Y. 2001. Caste sex ratios, sex linkage, and reproductive strategies in termites. *Insectes*
984 *soc* **48**: 224–230.
- 985 Romiguier J, Lourenco J, Gayral P, Faivre N, Weinert LA, Ravel S, Ballenghien M, Cahais V,
986 Bernard A, Loire E, et al. 2014. Population genomics of eusocial insects: the costs of a
987 vertebrate-like effective population size. *Journal of Evolutionary Biology* **27**: 593–
988 603.
- 989 Ross L, Blackmon H, Lorite P, Gokhman VE, Hardy NB. 2015. Recombination, chromosome
990 number and eusociality in the Hymenoptera. *Journal of Evolutionary Biology* **28**:
991 105–116.
- 992 Rueppell O, Kuster R, Miller K, Fouks B, Rubio Correa S, Collazo J, Phaincharoen M, Tingek S,
993 Koeniger N. 2016. A New Metazoan Recombination Rate Record and Consistently
994 High Recombination Rates in the Honey Bee Genus *Apis* Accompanied by Frequent
995 Inversions but Not Translocations. *Genome Biol Evol* **8**: 3653–3660.
- 996 Sarda S, Zeng J, Hunt BG, Yi SV. 2012. The Evolution of Invertebrate Gene Body Methylation.
997 *Mol Biol Evol* **29**: 1907–1916.
- 998 Seabold S, Perktold J. 2010. Statsmodels: Econometric and Statistical Modeling with Python.
999 In *Proceedings of the 9th Python in Science Conference* (eds. S. Van der Walt and J.
1000 Millman), pp. 92–96.
- 1001 Sherman PW. 1979. Insect Chromosome Numbers and Eusociality. *The American Naturalist*
1002 **113**: 925–935.
- 1003 Shi YY, Sun LX, Huang ZY, Wu XB, Zhu YQ, Zheng HJ, Zeng ZJ. 2013. A SNP Based High-Density
1004 Linkage Map of *Apis cerana* Reveals a High Recombination Rate Similar to *Apis*
1005 *mellifera*. *PLOS ONE* **8**: e76459.
- 1006 Siller S. 2001. Sexual selection and the maintenance of sex. *Nature* **411**: 689–692.

- 1007 Singhal S, Leffler EM, Sannareddy K, Turner I, Venn O, Hooper DM, Strand AI, Li Q, Raney B,
1008 Balakrishnan CN, et al. 2015. Stable recombination hotspots in birds. *Science* **350**:
1009 928–932.
- 1010 Sirviö A, Gadau J, Rueppell O, Lamatsch D, Boomsma JJ, Pamilo P, PAGE Jr. RE. 2006. High
1011 recombination frequency creates genotypic diversity in colonies of the leaf-cutting
1012 ant *Acromyrmex echinator*. *Journal of Evolutionary Biology* **19**: 1475–1485.
- 1013 Sirviö A, Johnston JS, Wenseleers T, Pamilo P. 2011a. A high recombination rate in eusocial
1014 Hymenoptera: evidence from the common wasp *Vespula vulgaris*. *BMC Genetics* **12**:
1015 95.
- 1016 Sirviö A, Pamilo P, Johnson RA, Page Jr Robert E, Gadau J. 2011b. ORIGIN AND EVOLUTION
1017 OF THE DEPENDENT LINEAGES IN THE GENETIC CASTE DETERMINATION SYSTEM OF
1018 POGONOMYRMEX ANTS. *Evolution* **65**: 869–884.
- 1019 Smukowski Heil CS, Ellison C, Dubin M, Noor MAF. 2015. Recombining without Hotspots: A
1020 Comprehensive Evolutionary Portrait of Recombination in Two Closely Related
1021 Species of *Drosophila*. *Genome Biology and Evolution* **7**: 2829–2842.
- 1022 Stapley J, Feulner PGD, Johnston SE, Santure AW, Smadja CM. 2017. Variation in
1023 recombination frequency and distribution across eukaryotes: patterns and
1024 processes. *Philosophical Transactions of the Royal Society B: Biological Sciences* **372**:
1025 20160455.
- 1026 Storer J, Hubley R, Rosen J, Wheeler TJ, Smit AF. 2021. The Dfam community resource of
1027 transposable element families, sequence models, and genome annotations. *Mobile
1028 DNA* **12**: 2.
- 1029 Templeton AR. 1979. Chromosome Number, Quantitative Genetics and Eusociality. *The
1030 American Naturalist* **113**: 937–941.
- 1031 Torres AP i, Höök L, Näsvalk K, Shipilina D, Wiklund C, Vila R, Pruisscher P, Backström N.
1032 2023. The fine-scale recombination rate variation and associations with genomic
1033 features in a butterfly. *Genome Res* **33**: 810–823.
- 1034 Trivers RL, Hare H. 1976. Haploidploidy and the Evolution of the Social Insect. *Science* **191**:
1035 249–263.
- 1036 Ventós-Alfonso A, Ylla G, Montañes J-C, Belles X. 2020. DNMT1 Promotes Genome
1037 Methylation and Early Embryo Development in Cockroaches. *iScience* **23**: 101778.
- 1038 Waiker P, de Abreu FCP, Luna-Lucena D, Freitas FCP, Simões ZLP, Rueppell O. 2021.
1039 Recombination mapping of the Brazilian stingless bee *Frieseomelitta varia* confirms
1040 high recombination rates in social hymenoptera. *BMC Genomics* **22**: 673.
- 1041 Wallberg A, Bunikis I, Pettersson OV, Mosbech M-B, Childers AK, Evans JD, Mikheyev AS,
1042 Robertson HM, Robinson GE, Webster MT. 2019. A hybrid de novo genome assembly

- 1043 of the honeybee, *Apis mellifera*, with chromosome-length scaffolds. *BMC Genomics*
1044 **20**: 275.
- 1045 Wallberg A, Glémin S, Webster MT. 2015. Extreme recombination frequencies shape
1046 genome variation and evolution in the honeybee, *Apis mellifera*. *PLoS Genetics* **11**:
1047 e1005189.
- 1048 Wallberg A, Han F, Wellhagen G, Dahle B, Kawata M, Haddad N, Simões ZLP, Allsopp MH,
1049 Kandemir I, De la Rúa P, et al. 2014. A worldwide survey of genome sequence
1050 variation provides insight into the evolutionary history of the honeybee *Apis*
1051 *mellifera*. *Nat Genet* **46**: 1081–1088.
- 1052 Wallberg A, Schöning C, Webster MT, Hasselmann M. 2017. Two extended haplotype blocks
1053 are associated with adaptation to high altitude habitats in East African honey bees.
1054 *PLoS Genetics* **13**: e1006792.
- 1055 Wang J, Chitsaz F, Derbyshire MK, Gonzales NR, Gwadz M, Lu S, Marchler GH, Song JS,
1056 Thanki N, Yamashita RA, et al. 2023. The conserved domain database in 2023.
1057 *Nucleic Acids Res* **51**: D384–D388.
- 1058 Wang X, Wheeler D, Avery A, Rago A, Choi J-H, Colbourne JK, Clark AG, Werren JH. 2013.
1059 Function and Evolution of DNA Methylation in *Nasonia vitripennis*. *PLoS Genet* **9**:
1060 e1003872.
- 1061 Watterson GA. 1975. On the number of segregating sites in genetical models without
1062 recombination. *Theoretical Population Biology* **7**: 256–276.
- 1063 Wilfert L, Gadau J, Schmid-Hempel P. 2007. Variation in genomic recombination rates
1064 among animal taxa and the case of social insects. *Heredity (Edinb)* **98**: 189–197.
- 1065 Winkler L, Moiron M, Morrow EH, Janicke T. 2021. Stronger net selection on males across
1066 animals eds. P.J. Wittkopp and L. Holman. *eLife* **10**: e68316.
- 1067 Winston ML. 1991. *The Biology of the Honey Bee*. Revised edition. Harvard University Press,
1068 Cambridge, Mass.
- 1069 Wu T-C, Lichten M. 1994. Meiosis-Induced Double-Strand Break Sites Determined by Yeast
1070 Chromatin Structure. *Science* **263**: 515–518.
- 1071 Yang S, Wang L, Huang J, Zhang X, Yuan Y, Chen J-Q, Hurst LD, Tian D. 2015. Parent–progeny
1072 sequencing indicates higher mutation rates in heterozygotes. *Nature* **523**: 463–467.
- 1073 Zhang C, Dong S-S, Xu J-Y, He W-M, Yang T-L. 2019. PopLDdecay: a fast and effective tool for
1074 linkage disequilibrium decay analysis based on variant call format files.
1075 *Bioinformatics* **35**: 1786–1788.

1076

1077 **Figure Legends:**

1078

1079 **Figure 1.** Genome-wide decay of LD measured as r^2 versus distance (bp) between SNPs for
1080 the two termite species (*M. bellicosus*, dark red; *C. secundus*, yellow) and honey bees (*A.*
1081 *mellifera scutellata*, blue; data from Wallberg et al. 2017).

1082 **Figure 2.** Variation in recombination rate estimated as ρ /kbp across representative genomic
1083 scaffolds in a) *M. bellicosus* and b) *C. secundus*. Estimates of ρ /kbp are calculated in 10 kbp
1084 and 100 kbp windows.

1085 **Figure 3.** Cumulative plot of proportion of recombination events versus proportion of the
1086 genome for the two termite species *M. bellicosus* and *C. secundus* compared to the honey
1087 bee *A. mellifera* (Wallberg et al. 2015). Dashed lines show the proportion of the genome
1088 where 50 % of the recombination occurs, which for *M. bellicosus* is 0.4 %, *C. secundus* is 0.2
1089 %, and *A. mellifera* is 32 %.

1090 **Figure 4.** PRMD9 structure and predicted zinc-finger motifs in the *M. bellicosus* and *C.*
1091 *secundus* genomes. A) Predicted structure of the PRDM9 protein sequence in *C. secundus*. B)
1092 Predicted structure of the *PRDM9* gene in *M. bellicosus* identified by homology searches.
1093 Exons and conserved functional domains are marked. The mapped exons from
1094 *Zoothermopsis nevadensis* are also shown. C) Structure of *PRDM9* gene in *C. secundus*.
1095 Exons and conserved functional domains are marked. D) Predicted zinc finger binding motif
1096 in *M. bellicosus*, E) Predicted zinc finger binding motif in *C. secundus*.

1097 **Figure 5.** Boxplots showing variation in levels of CpG_{O/E} and recombination rate (ρ /kbp; rho)
1098 in genic and flanking regions in the *M. bellicosus* and *C. secundus* genomes. The differences
1099 between all categories are significant.

1100 **Figure 6.** Boxplots showing variation in levels of CpG_{O/E} and recombination rate (ρ /kbp) in
1101 the coding region of genes in the *M. bellicosus* and *C. secundus* genomes classified according
1102 to their patterns of gene expression (Q = queen-biased, K = king-biased, W = worker-biased,
1103 F = female-biased, R = reproductive-biased).

1104

1105

1106 **Table 1.** Estimates of levels genetic variation, effective population size and recombination rate in two termite species.

1107

Species	Assembly length (Mb)	No. SNPs	θ_w /bp	μ bp ⁻¹ gen ⁻¹	N_E	LDhat		LDhelmet	
						ρ /kb	r (cM/Mb)	ρ /kb	r (cM/Mb)
<i>M. bellicosus</i>	1,139	5,581,662	0.14%	2.7 x 10 ⁻¹⁰	1,278,982	1.69	0.033	4.28	0.084
				4.5 x 10 ⁻⁹	76,876				1.392
				8.1 x 10 ⁻⁹	42,898				2.494
<i>C. secundus</i>	992	15,037,468	0.44%	2.7 x 10 ⁻¹⁰	4,080,725	4.85	0.030	16.39	0.100
				4.5 x 10 ⁻⁹	245,280				1.671
				8.1 x 10 ⁻⁹	136,869				2.994

1108 θ_w /bp - Watterson's θ per base pair

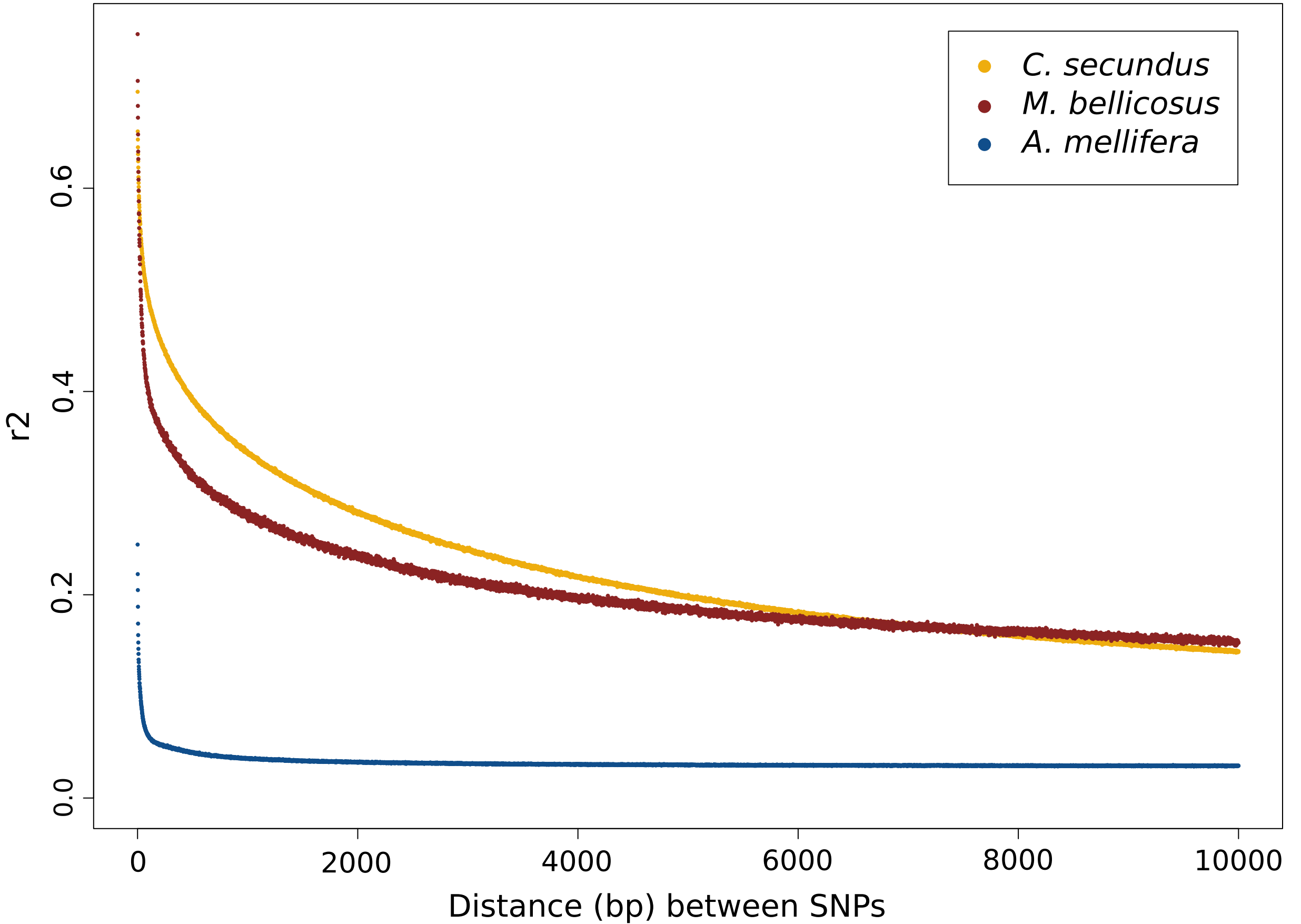
1109 ρ /kbp - population recombination parameter, ρ , per kilobase

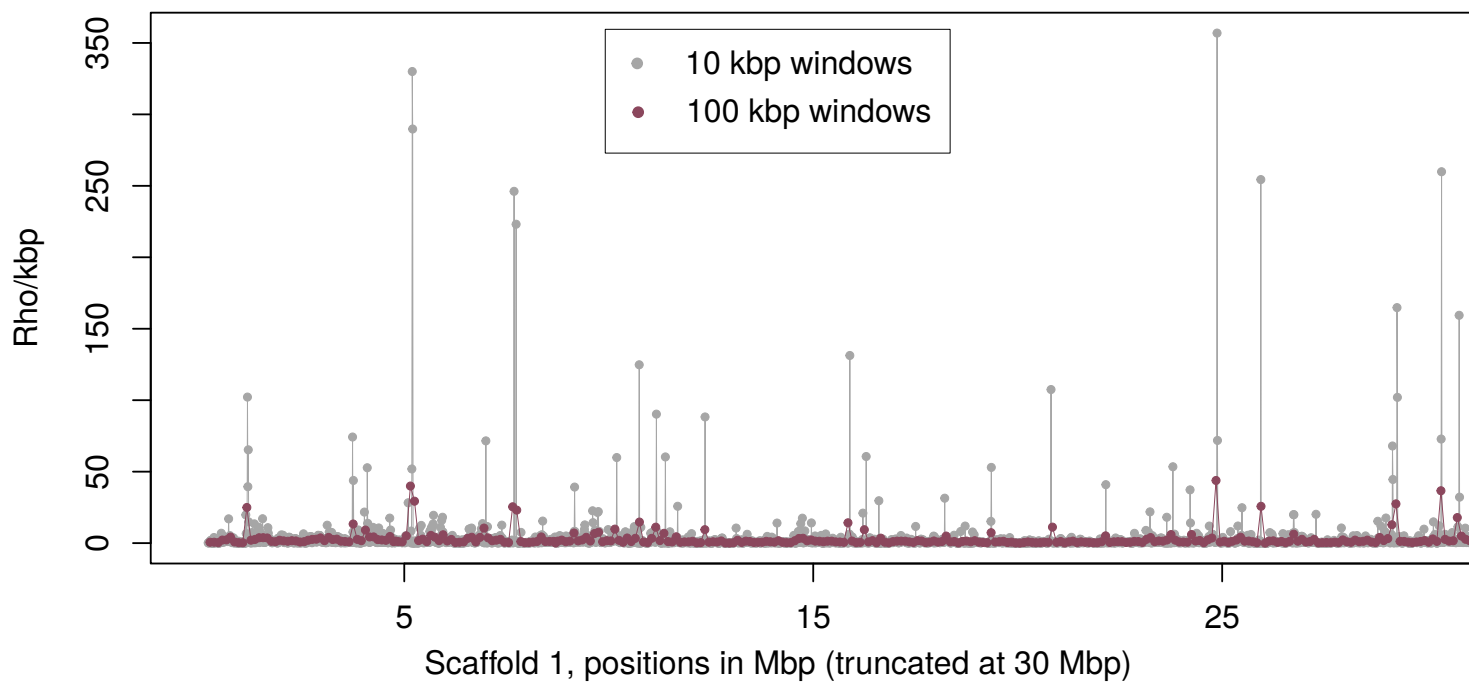
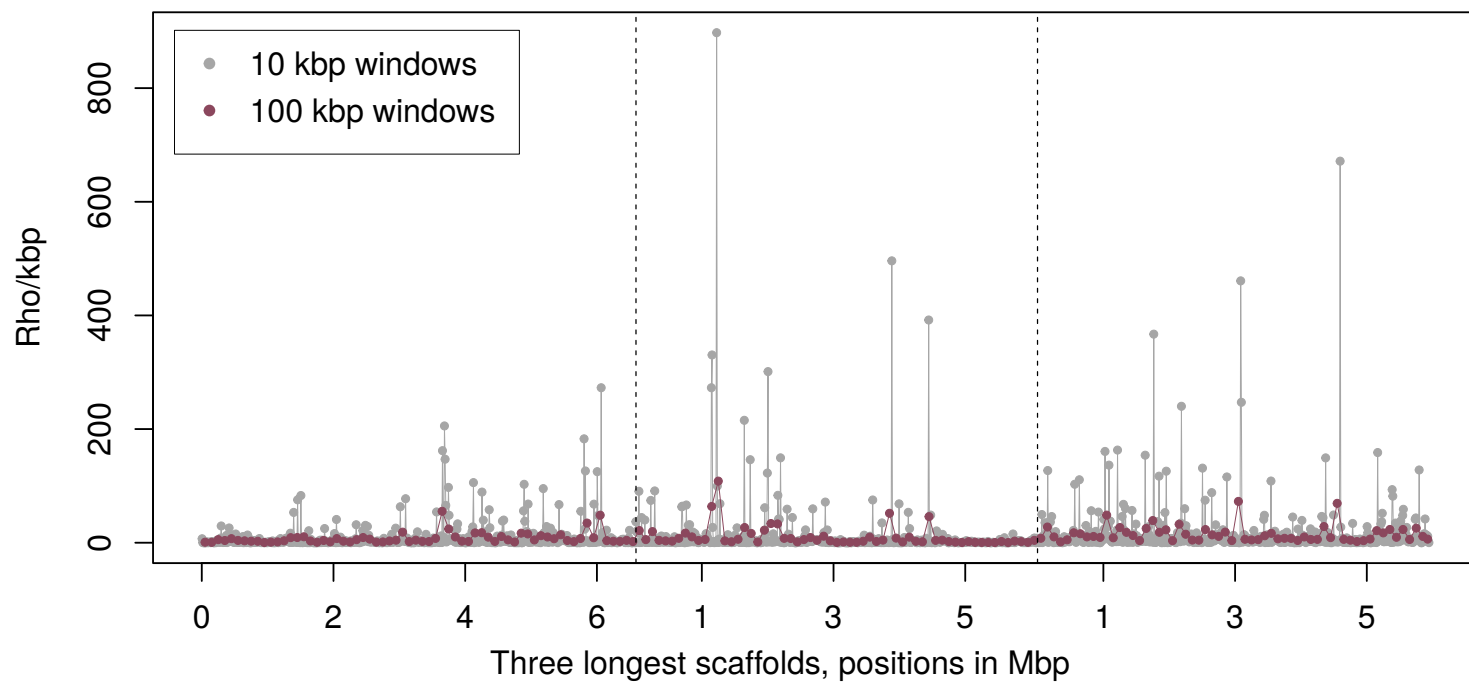
1110 μ bp⁻¹ gen⁻¹ - mutation rate per base pair per generation taken from literature. Estimates correspond to *Acyrtosiphon pisum* (2.7 x 10⁻¹⁰), *Drosophila*
 1111 *melanogaster* (4.5 x 10⁻⁹) and *Drosophila pseudoobscura* (8.1 x 10⁻⁹)(Lynch et al. 2023).

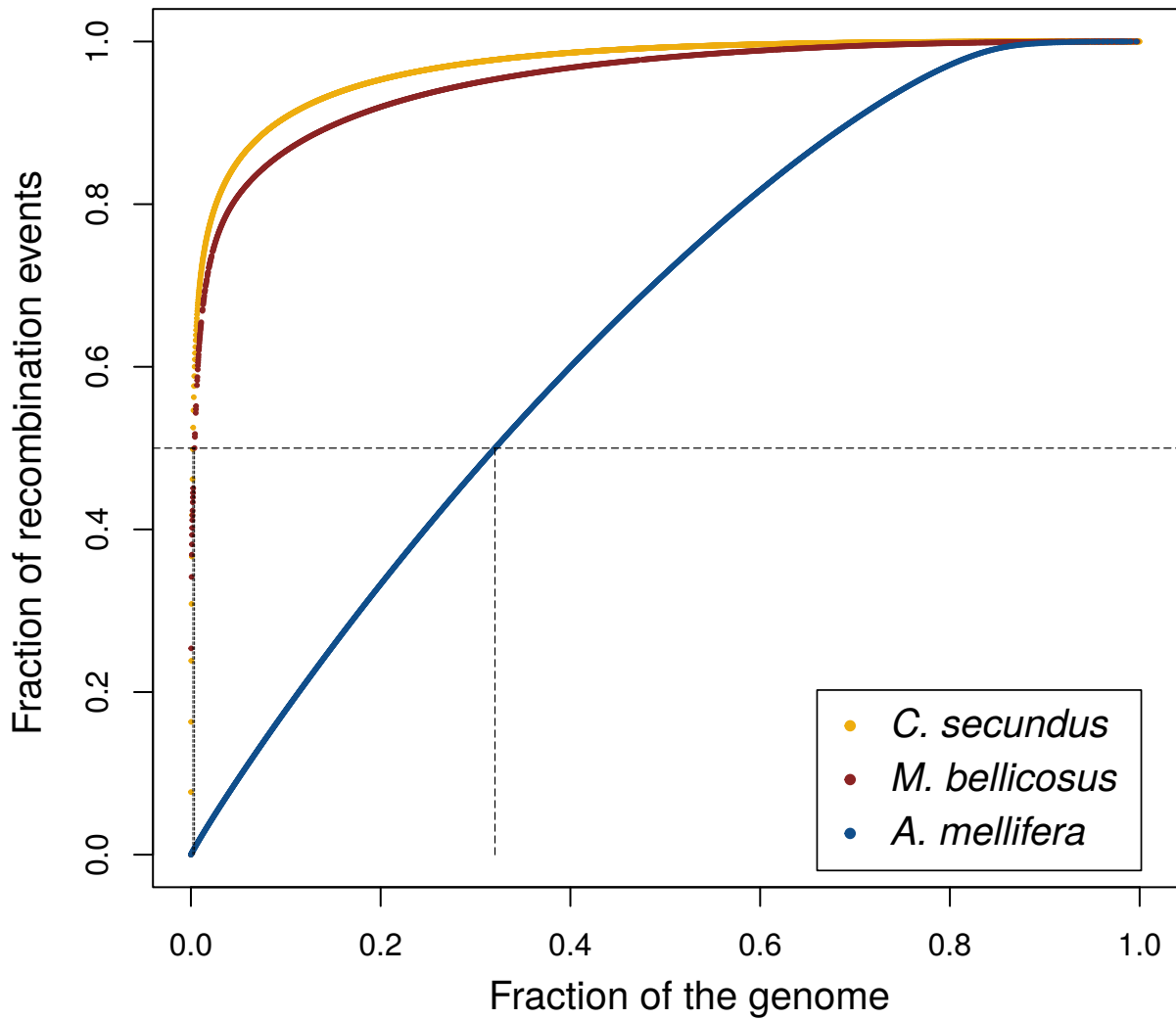
1112 N_E - effective population size

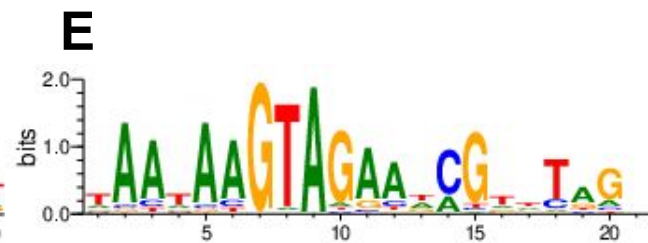
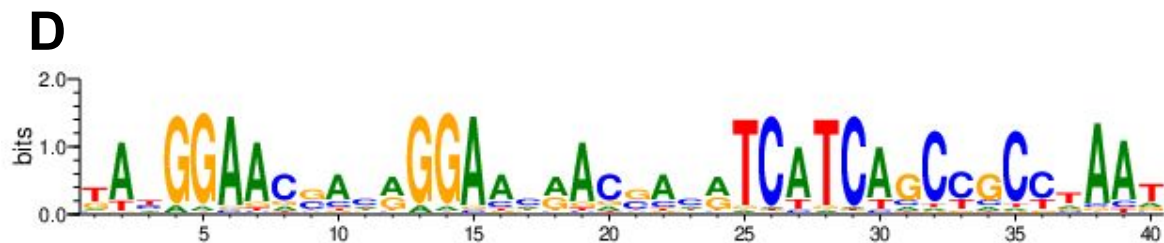
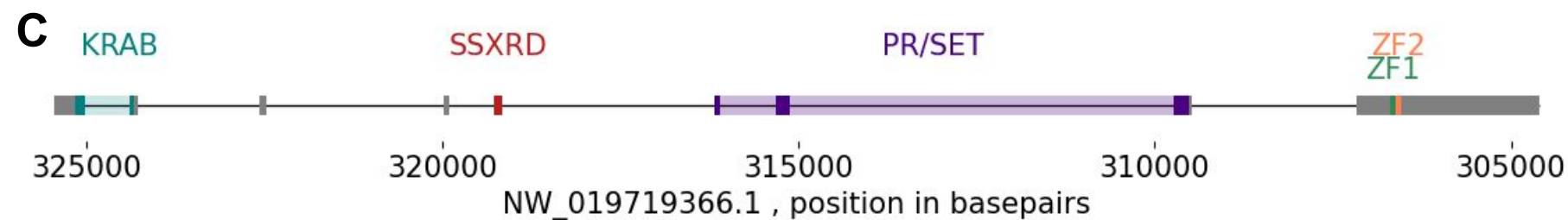
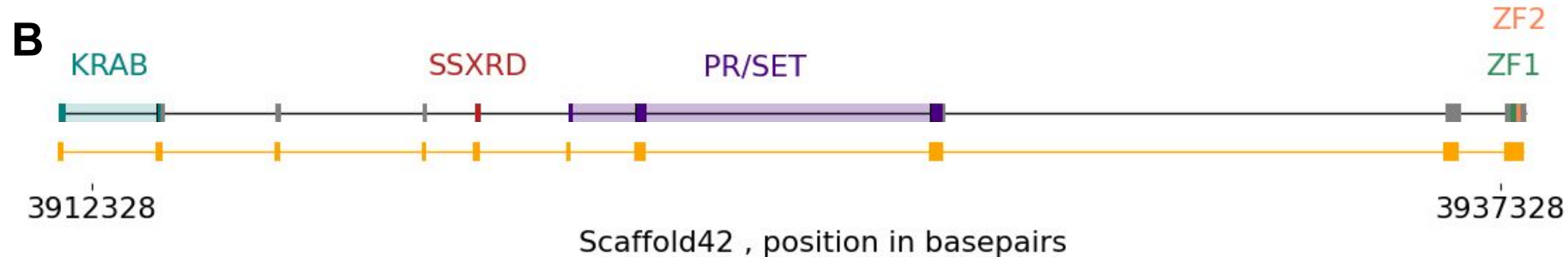
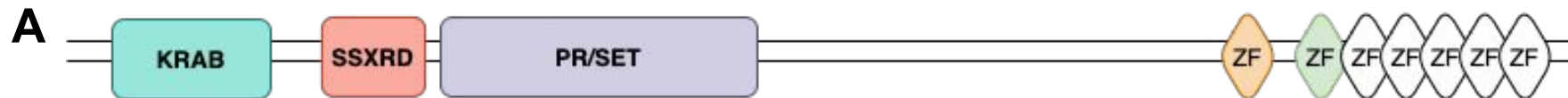
1113 r (cM/Mb) - recombination rate in centimorgans per megabase

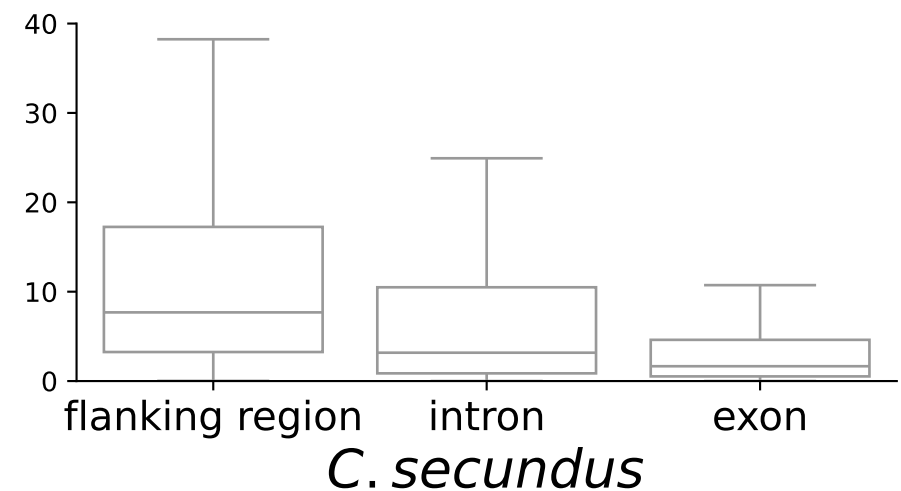
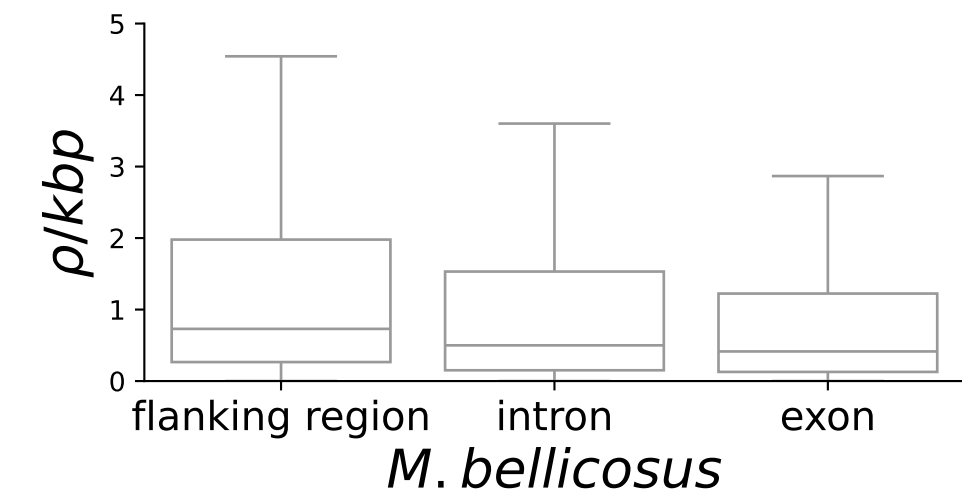
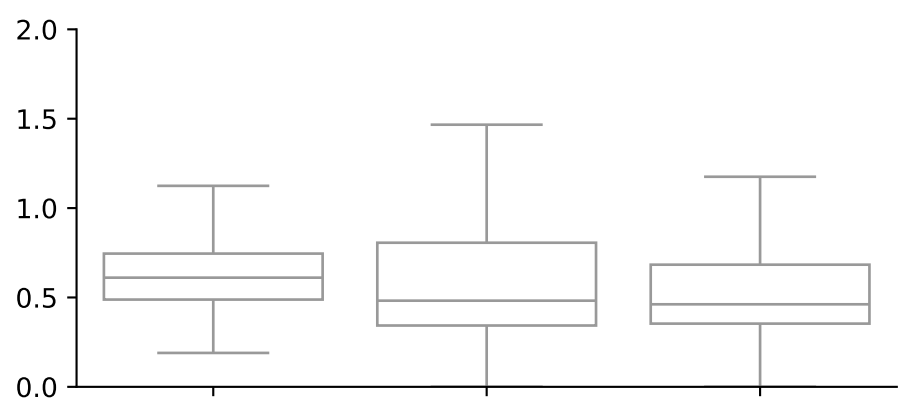
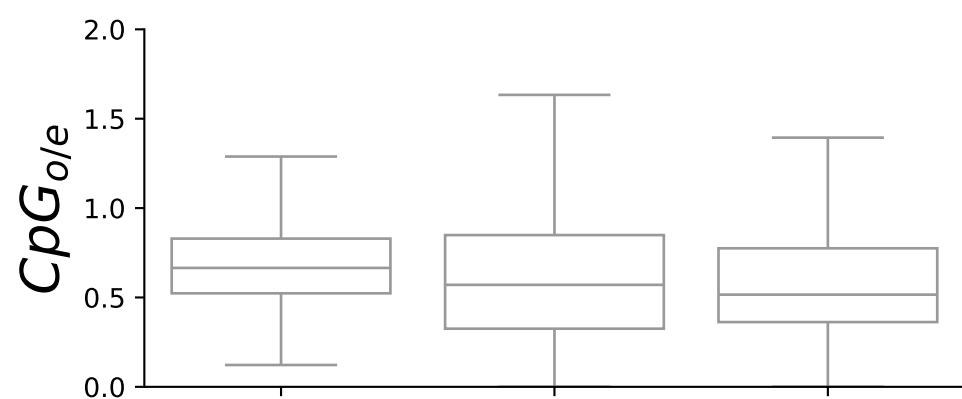
1114

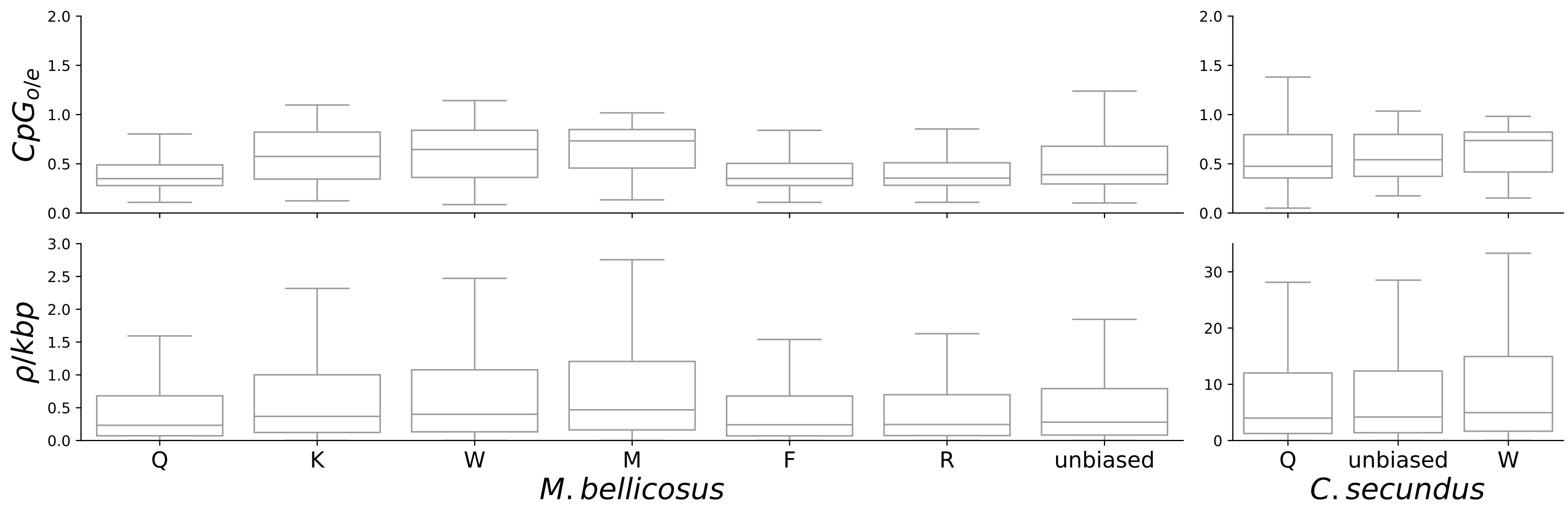


A*M. bellicosus***B***C. secundus*











Unexpectedly low recombination rates and presence of hotspots in termite genomes

Turid Everitt, Tilman Ronneburg, Daniel Elsner, et al.

Genome Res. published online March 20, 2025

Access the most recent version at doi:[10.1101/gr.279180.124](https://doi.org/10.1101/gr.279180.124)

Supplemental Material <http://genome.cshlp.org/content/suppl/2025/04/10/gr.279180.124.DC1>

P<P Published online March 20, 2025 in advance of the print journal.

Accepted Manuscript Peer-reviewed and accepted for publication but not copyedited or typeset; accepted manuscript is likely to differ from the final, published version.

Creative Commons License This article is distributed exclusively by Cold Spring Harbor Laboratory Press for the first six months after the full-issue publication date (see <https://genome.cshlp.org/site/misc/terms.xhtml>). After six months, it is available under a Creative Commons License (Attribution-NonCommercial 4.0 International), as described at <http://creativecommons.org/licenses/by-nc/4.0/>.

Email Alerting Service Receive free email alerts when new articles cite this article - sign up in the box at the top right corner of the article or [click here](#).



To subscribe to *Genome Research* go to:
<https://genome.cshlp.org/subscriptions>
